Proof-of-Theft: Dynamic Graph-Based Fingerprinting of In-Browser Cryptomining

Tanapoom Sermchaiwong
The Hong Kong University of Science and Technology, China

Jiasi Shen[1]
The Hong Kong University of Science and Technology, China

Abstract

The decentralized and unregulated nature of cryptocurrencies, combined with their monetary value, has made them a vehicle for various illicit activities. One such activity is cryptojacking, an attack that uses stolen computing resources to mine cryptocurrencies without consent for profit. In-browser cryptojacking malware exploits high-performance web technologies such as WebAssembly to mine cryptocurrencies directly within the browser without file downloads. Although existing methods for cryptomining detection report high accuracy and low overhead, they are often susceptible to various forms of obfuscation, and due to the limited variety of cryptomining scripts in the wild, standard code obfuscation methods present a natural and appealing solution to avoid detection. To address these limitations, we propose using instruction-level data-flow graphs to detect cryptomining behavior. Data-flow graphs offer detailed structural insights into a program's computations, making them suitable for characterizing proof-of-work algorithms, but they can be difficult to analyze due to their large size and susceptibility to noise and fragmentation under obfuscation. We present two techniques to simplify and compare data-flow graphs: (1) a graph simplification algorithm to reduce the computational burden of processing large and granular data-flow graphs while preserving local substructures; and (2) a subgraph similarity measure, the *n-fragment inclusion score*, based on fragment inclusion that is robust against noise and obfuscation. Using data-flow graphs as computation fingerprints, our detection framework PoT (*Proof-of-Theft*) was able to achieve high detection accuracy against standard obfuscations, outperforming existing detection methods.

2012 ACM Subject Classification Software and its engineering → Dynamic analysis; Security and privacy → Web application security

Keywords and phrases software security, cryptocurrency, malware detection, dynamic analysis, data-flow graph

Digital Object Identifier 10.4230/LIPIcs.ECOOP.2026.25

Supplementary Material *Software (Source Code and Dataset)*: `https://zenodo.org/records/18496931`
Software (ECOOP 2026 Artifact Evaluation approved artifact): `https://doi.org/10.4230/DARTS.12.1.19`

Funding This work was supported in part by the Hong Kong Research Grants Council (Project No. 26216025) and the Alibaba Group (through the Alibaba Innovative Research Program). The views expressed in this work are those of the authors and do not necessarily reflect the views of the funding agencies.

Acknowledgements We thank the anonymous reviewers and the other members at the Software Automation Research Group at HKUST for their insightful and helpful comments.

[1] Corresponding Author

1 Introduction

A cryptocurrency is a decentralized peer-to-peer digital exchange system that functions as a currency without a central authority [50]. The absence of a central governing body and the promise of freedom and resistance to censorship have led to widespread initial adoption of cryptocurrencies. Combined with the speculative nature of the market, this has created an enormous growth in demand [16]. The staggering increase in the monetary value of many cryptocurrencies in recent years has made cryptomining a potential source of income derived from computing power [24]. In some cases, stolen computing resources are used to generate profits through unauthorized mining. The use of unauthorized computational power to mine cryptocurrency without consent is called *cryptojacking*, and this attack happens on all scales of computing systems, from large data centers to small personal platforms such as web browsers and IOT devices [3, 64]. As recently as 2024, instances of cryptojacking attacks have caused significant monetary damages to organizations such as the United States government [57] and many financial institutions [41].

In-browser cryptojacking is a recently emerged type of fileless malware that is difficult to detect in the traditional framework of malware detection [14]. Recent studies have demonstrated the prevalence of in-browser cryptojacking on popular websites based on their analyses of top-ranking websites [23, 52, 65, 68]. In-browser cryptojacking is enabled partially by new technologies such as WebAssembly (Wasm) [70] and WebWorkers [49], which were introduced to facilitate high-performance applications to run on web browsers, delivering cryptominers filelessly through scripts on a webpage. In fact, previous works showed that most of these miners are implemented in Wasm [42]. Popular services such as CoinHive facilitated this process by providing mining scripts and mining pools as an alternative source of revenue for websites, and although the CoinHive service was shut down in 2019, multiple studies indicate that in-browser cryptojacking is still prevalent in the wild [23, 52, 65].

To prevent theft of computing resources, various techniques have been proposed to detect and prevent cryptominers from running in browsers. These include traditional methods such as domain name blocking and keyword blacklists [33, 37, 32], as well as those involving more advanced analysis such as semantic instruction counting [69, 7, 15], CPU, memory, and network traffic monitoring [58, 36, 38], and static approaches based on machine learning and deep learning [53, 59]. Although existing detection methods report high accuracy, they are often susceptible to obfuscation [6, 30, 69]. For example, proxies, dynamically generated domain names, and encrypted WebSocket communication can render blacklists and network-based detection methods ineffective. Statistical distributions of instructions can be skewed by performance throttling and the insertion of spurious instructions. CPU and memory event monitoring is susceptible to noise from other processes or web pages [28]. Deep learning-based approaches such as those proposed by MINOS [53] and WASim [59] have been shown to perform poorly on obfuscated and diversified binaries [30, 6]. These obfuscations are easy to apply with access to the source code, thereby restricting the usefulness of prior approaches due to the ease with which they are bypassed. There remains a large gap in detecting obfuscated miners effectively.

Cryptomining in a single browser is often too slow to generate profit since the probability of calculating the correct hash in a reasonable amount of time is minuscule, and the solution is usually to mine cryptocurrency as a part of a larger pool, where profit from any correctly mined hash is shared among the participants. This suggests that in-browser cryptojacking is only feasible on economies of scale, and numerous studies support this hypothesis, indicating that a large majority of in-browser cryptomining scripts originate from a limited number of services (e.g., CoinHive, CoinImp, JSECoin) that provide the necessary infrastructure, such as mining scripts and pools [65, 68, 38]. The small diversity of cryptominers deployed on a large number of platforms makes obfuscation an attractive solution to evade detection. Therefore, there is a need for better detection methods of obfuscated cryptomining malware.

In this paper, we propose PoT (*Proof-of-Theft*), a new approach to detect obfuscated cryptomining malware based on the following key insights. Fundamentally, a cryptominer performs calculations to validate transactions on the blockchain. In most proof-of-work schemes, this entails repeated hashing of a block of data to generate a hash satisfying an arbitrary but difficult property [50]. This repetitive computation is an intrinsic property of a proof-of-work scheme. To characterize the computations performed by an algorithm, instruction-level data-flow graphs provide a structured and comprehensive view of computation that is difficult to manipulate. We hypothesize that the data-flow graphs provide us with a direct view of a cryptominer's core characteristic. Moreover, code obfuscators are known to operate within certain boundaries [45], suggesting that there are a limited number of transformations they can make to the data-flow properties of a program.

Instruction-level data-flow graphs are difficult to compare due to their sizes and susceptibility to noise and fragmentation. To enable their use in cryptomining detection, we propose a set of graph analysis techniques consisting of: (1) a graph simplification algorithm to generate computation fingerprints from data-flow graphs; and (2) a subgraph similarity measure to search for malicious behavior in fingerprints. We demonstrate that PoT outperforms the state-of-the-art in cryptominer detection under various obfuscations. To the best of our knowledge, this study is the first to utilize instruction-level data-flow graphs in detecting cryptominers.

In summary, this paper makes the following three major contributions:

- We present a novel algorithm to simplify large repetitive data-flow graphs that preserves local substructures, enabling large and granular data-flow graphs to be used in cryptomining detection.
- We introduce a new subgraph similarity measure, *n-fragment inclusion score*, to compare graphs based on inclusion that is resilient against noise, fragmentation, and obfuscation.
- We implement and evaluate PoT for detecting WebAssembly cryptominers on a sample of 29 real-world web applications, 6 cryptominers, and 30 obfuscated cryptominers, showing the effectiveness of instruction-level data-flow graphs in obfuscation resistant detection of cryptojacking.

2 Background and Motivation

In this section, we present essential concepts, motivation, and a review of the current literature.

2.1 Cryptomining and Proof-of-Work Schemes

To ensure the validity of transactions on a blockchain, participants are encouraged to validate the authenticity of new transactions [50]. Cryptocurrency systems employ a consensus mechanism to prevent a single actor from validating invalid transactions using multiple fake nodes. Our methodology focuses on the most ubiquitous form [5] of consensus used by cryptocurrencies, *Proof of Work*, in which validators (miners) are required to provide proof that they possess a certain amount of computing resources before validating new blocks. Miners are rewarded for each new block they successfully validate, and this process is commonly referred to as cryptomining as it allows miners to generate income in exchange for performing resource-intensive computations.

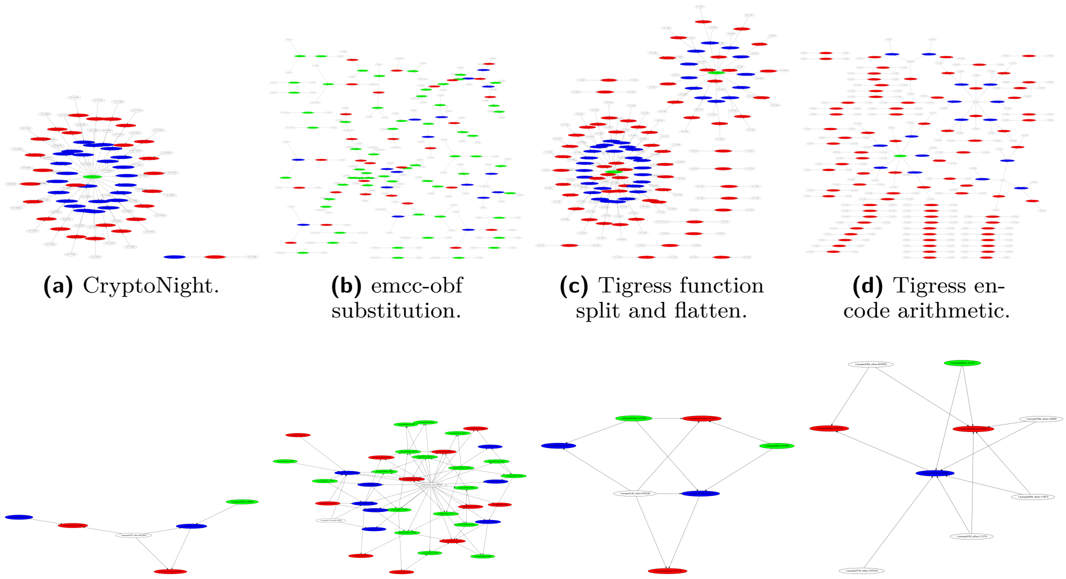

(a) CryptoNight. **(b)** emcc-obf substitution. **(c)** Tigress function split and flatten. **(d)** Tigress encode arithmetic. **(e)** Simplified CryptoNight. **(f)** Simplified emcc-obf substitution. **(g)** Simplified Tigress function split and flatten. **(h)** Simplified Tigress encode arithmetic.

Figure 1 (CryptoNight data-flow graphs) Visualizations of the data-flow graphs of the CryptoNight algorithm in its original and simplified forms and under different obfuscations. Figure (a) shows the original graph, while (b) to (d) show three obfuscated versions. Figures (e) to (h) show the simplified versions of (a) to (d). Red, green, and blue vertices represent `and`, `xor`, and `shr` instructions respectively. Other instructions are not traced but may appear as data origin in the graph as uncolored vertices.

The computationally intensive task required to verify a block usually involves computing a hash of a block combined with a random value until a hash with an arbitrary but difficult property is found. Several proof-of-work algorithms have been implemented since the widespread adoption of cryptocurrencies. Notable are ASICs and GPU resistant [18] currencies such as Monero [48], MintMe [47], and other CryptoNight [21] currencies, which are commonly used for in-browser cryptojacking [65, 19] since they can be efficiently mined on the CPU through WebAssembly. Our experiments focus on this class of miners.

A fundamental characteristic of most proof-of-work algorithms is an extensive amount of repetitive computation arising from repeated hashing. In a data-flow graph where each execution of an instruction represents a unique vertex, redundant computations emerge as repeated subgraphs representing the same computation performed many times. This key insight allows us to compress the graph into a much smaller form while preserving local semantics of a program. Figure 1a and Figure 1e depict graphs of the CryptoNight algorithm before and after simplification, respectively. We will discuss the details and construction of these graphs in later sections.

2.2 Cryptojacking Detection

Numerous studies have proposed highly accurate detection systems to address cryptojacking malware. These systems utilize one or more of the following program features: network behavior, resource and performance metrics, semantic instruction count, and the program binary file. We discuss these systems in the following section.

Network Behavioral Detection. Several network detection methods have been proposed for large-scale and platform-agnostic detection of cryptojacking. Caprolu et al. [13] and Pastor et al. [56] proposed the use of network flow features to classify and detect cryptominers which communicate with a mining pool. MineCap [54] presented a similar idea using super-incremental learning to reduce the training burden. XMR-Ray [60] proposed more refined network-flow features specific to the Stratum pool mining protocol, and employed one-class classification techniques to allow the model to be trained using only mining traffic.

While these systems report good detection rates and scalability, they are limited to the specific mining pool protocol on which they were trained. The authors of XMR-Ray noted that hand-crafted obfuscations and deviations from the expected protocol can affect the detection rates of these methods. Deviating from a mining pool protocol is a much easier task than changing the underlying cryptomining algorithm, which requires a revision to the blockchain protocol, and hence network-based detection methods require less effort to evade.

Resource and Performance Metrics. Researchers have proposed cryptomining detection based on CPU, memory, and other resource consumption metrics. These methods employ side channels to detect the secondary effects of proof-of-work computations. Wu et al. [72] and Gomes and Correia [28] proposed machine learning classification of cryptominers based on CPU usage metrics. DeCrypto Pro [46] introduced a more comprehensive set of performance counters for classification by reading processor, memory, and disk metrics. Outguard [38] and CoinSpy [36] included network features and statistics from the JavaScript engine in addition to raw performance data. Gangwal and Conti [26] proposed a magnetic side-channel by profiling magnetic field emission of a processor during cryptomining.

The authors of these studies noted several drawbacks of using performance metrics and side channels. These systems are sensitive to noise from external processes that run concurrently. They also require administrator privileges to monitor performance counters and system events. In addition, miners can restrict their behavior by throttling or performing arbitrary tasks concurrently to manipulate performance metrics. Coinspy [36] and Outguard [38] tried to fix these drawbacks by incorporating both network and performance metrics.

Semantic Instruction Count. The results of Seismic [69] indicate that cryptomining behavior and proof-of-work algorithms can be differentiated at the semantic instruction level. Their findings highlight the significance of a few binary instructions such as `and`, `xor`, and `shr` in cryptominers. They proposed a detection method based on the statistical distribution of instructions in dynamically collected execution traces. Carlin et al. [15] performed a similar analysis by training machine learning models on opcode distribution. MineSweeper [42] hand-crafted algorithm-specific signatures using instruction count analysis. MineThrottle [7] refined this approach by profiling only a small number of frequently executed blocks of code and checking the distribution of instructions within these blocks.

The detection of cryptominers based on instruction counts can be easily circumvented by inserting spurious instructions to skew the distribution. While MineThrottle [7] tries to address this issue by profiling only frequently executed code blocks, blocks can be duplicated to hide their true frequency or divided into smaller blocks to dilute the incriminating instructions. The method we propose in this paper is built on the foundation of semantic instruction distribution, but we also incorporate the structure of data-flow to improve the robustness of our detection method. The graph in Figure 1a provides a rough intuition of how this is done, where the edges represent data-flow, and the vertices represent instructions and are color coded red, green, blue for “and”, “shr”, and “xor” instructions, respectively.

Binary File Analysis. Romano and Wang [59] proposed WASim, a method to classify WebAssembly binaries using features and metadata extracted from Wasm binary files to train machine learning models. The authors of MINOS [53] discovered that WebAssembly cryptojacking binaries often look similar when represented directly as grayscale images and proposed a convolutional neural network classifier on image representations of the binaries. Although they report high detection rates, this method is not robust because the WebAssembly binary format contains sections with debugging information which can grow arbitrarily large, allowing the image data to be modified arbitrarily. Cabrera-Arteaga et al. [11] and Harnes and Morrison [30] demonstrated that MINOS is also vulnerable to several forms of obfuscation, which is supported by our experimental results.

The body of prior work indicates that there is room for improvement in cryptojacking malware detection that is resilient against obfuscation and evasion.

2.3 Resource Graphs in Malware Detection

Resource graphs provide rich information on the behavior of a program, and as such, a large body of work exists on the use of graphs in detecting malicious software. Hu et al. [34] designed a system called SMIT which uses approximate graph edit distances of function-call graphs to compute the K nearest neighbors in a malware database. Although they concluded that function-call graphs are less susceptible to obfuscations, many tools have since been developed to perform sophisticated transformations on functions [20, 35]. Kinable et al. [40] proposed similar techniques to cluster call-graphs using approximate edit distance and density-based clustering (DBSCAN).

Park et al. [55] defined the similarity measure *maximal common subgraph* that is used to classify system call graphs by comparing them to those generated by malicious software. The normalized similarity of two graphs is the ratio between the size of the maximal shared subgraph and the larger of the two graphs. Although this concept of similarity resembles the subgraph similarity we propose in this paper, our measure focuses on smaller fragments of the subgraph to be more resistant to fragmentation and computationally feasible on large graphs. Hisham et al. [1] utilized graph algorithmic properties such as density, shortest path, diameter, radius, and other centrality measures to construct features from control flow graphs, which are classified using machine learning. Yamaguchi et al. [74] introduced a novel representation of source code called *code property graph*, which merges abstract syntax trees, control flow graphs, and program dependence graphs into a single structure. The combined data structure can be mined effectively to discover vulnerabilities in the program.

Later works also adopted deep learning techniques to classify resource graphs. For example, Gao et al. [27] demonstrated the effectiveness of graph convolutional networks in detecting android malware based on their API usage graphs. Anderson et al. [2] presents the only study we know of that uses instruction-level resource graphs to classify malicious software behavior. They use the adjacency of instructions in a dynamic execution trace to construct a Markov chain of assembly instructions, which are classified using graph kernels and machine learning.

The body of existing work on the usage of resource graphs in malware detection fails to address the challenges of detecting obfuscated cryptojacking malware. High-level system-call and API usage graphs do not provide much insight into the numerical computation of cryptominers. Furthermore, function call graphs and control flow graphs are trivially obfuscated using standard obfuscators such as Tigress [20] and OLLVM [35].

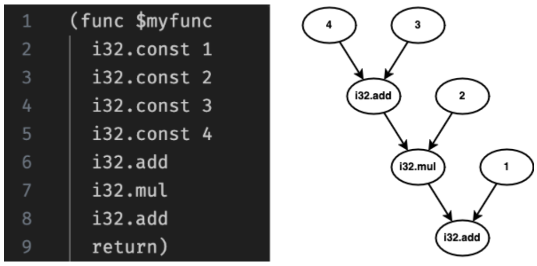

Figure 2 A short WebAssembly function in text format alongside its data-flow graph.

At the instruction level, resource graphs become significantly larger, making them much more challenging to analyze, as can be seen in the first row of Figure 1. The difficulty in utilizing instruction traces lies in simplifying massively granular information in a meaningful way and comparing the extracted features. The method proposed by Anderson et al. [2] to analyze instruction traces captures only the adjacency of instructions rather than the underlying data flow, which could be vulnerable to instruction reordering. Most importantly, the Markov chain representation does not effectively convey local substructures in the data-flow graphs, making it difficult to uncover superimposed computation. The current literature lacks a way to simplify instruction-level data flow graphs and compare them effectively. The techniques we proposed in this paper allow us to exploit these graphs which have never been explored in malware detection.

Finally, machine learning techniques are less suitable than fingerprinting methods due to the limited diversity of cryptominers [65, 68] and mining algorithms [5]. The results of Tekiner et al. [65] suggest that the large number of mining samples used in prior machine learning studies are likely duplicate cryptominer samples originating from a small number of service providers mining a few select cryptocurrencies. In the remainder of this study, we propose a method of simplifying large graphs while preserving repetitive local features. Examples of simplified graphs are visualized in Figure 1e-1h. We also define a novel notion of subgraph similarity that captures local graph properties and is resistant to obfuscation. Our paper represents the first step in comprehensively utilizing instruction-level data-flow graphs in cryptominer detection.

2.4 WebAssembly

WebAssembly (Wasm) is a low-level bytecode format designed to run at near-native performance on a wide variety of systems, providing a platform to deploy demanding software on the web [29]. While Wasm has seen gradual adoption [25, 17], recent studies indicate that it is still largely used for illicit purposes such as cryptojacking [51, 39]. Wasm presents an exciting future for delivering fast and energy-efficient applications through the web, but more studies need to be conducted on its security implications and mitigation.

An important property of WebAssembly for our analysis is that it operates as a stack machine. A function consists of a sequence of instructions that manipulate values on an operand stack, popping arguments and pushing results to the stack. An example WebAssembly snippet and the corresponding data-flow graph are presented in Figure 2. The details of our instrumentation are described in Section 5.

3 Threat Model and Solution Outline

In this study, we consider malicious web pages which mine cryptocurrency in the background. We assume that the majority of the proof-of-work algorithm is implemented in WebAssembly, which is the case for most cryptojacking scripts in the wild based on previous studies [38, 51, 42]. The attacker may mine with or without a pool, and protocol communications may be subject to any obfuscation. The web page may employ throttling or perform arbitrary tasks concurrently, and the WebAssembly binary may be subjected to standard code obfuscation and anti-analysis transformations. We assume that the detector has full access to the browser and is able to collect instruction traces of all WebAssembly execution.

A brief outline of our solution is as follows. First, we collect a sample of known cryptominers and record their data-flow graphs (Figure 1a), which are simplified by Algorithm 1 into fingerprints in our threat database (Figure 1e). In our experiment, this database consists of the 6 cryptominer samples described in Table 1 later. In a real-world deployment, the database is likely much larger. For each unknown sample to be tested, we also record and simplify their data-flow graphs into fingerprints. Finally, we check whether any malicious fingerprint in the database has a high subgraph similarity score to the sample fingerprint using Algorithm 2. If there is a match according to our threshold, the sample is classified as a cryptominer. Figure 1 should provide a general idea of how data-flow graphs might look before and after being simplified. Figure 3 will later provide a more detailed description of the simplification algorithm.

4 Graph Analysis

In this section, we describe our algorithms in detail. Our analysis is motivated by the observation that proof-of-work algorithms perform large amounts of repetitive and artificial computation. In data-flow graphs of dynamic single assigned variables, redundant computations emerge as regular substructures, allowing us to compress the graph into a much smaller form while preserving local semantics by combining these structures until there is little to no repetition remaining. Since the graphs represent computation at a very low abstraction level, we hypothesize that it should also maintain a degree of similarity between equivalent programs, even under obfuscation. First, we introduce our method of simplifying large graphs based on the aforementioned observations, then we define a new subgraph similarity measure capable of discovering similarities between seemingly different graphs of equivalent programs.

4.1 Instruction Level Data-Flow Graphs in WebAssembly

By treating each execution of a WebAssembly instruction as a distinct variable and capturing the flow of data between them, we create a directed acyclic graph with no multi-edges where the runtime variables are single-assigned. This graph represents the flow of data between executions of instructions in the program. The directed acyclic property is used throughout our design. To reduce the instrumentation overhead and computation load, we may record only data-flow into certain instructions of interest in the domain of our malware. Based on the results of Wang et al. [69], the use of three binary instructions, `and`, `shr`, and `xor`, is characteristic of cryptomining behavior. We elect to instrument only these three instructions to reduce computational burden in comparing graphs.

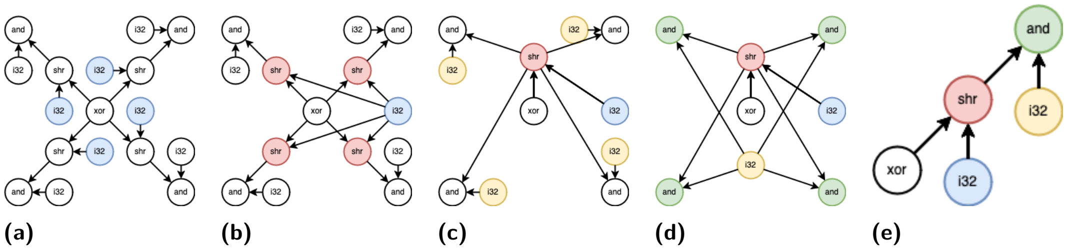

Figure 3 A step-by-step reduction of the CryptoNight graph. The root vertices of isomorphic subgraphs are highlight and merged at each step.

4.2 Fingerprinting Through Graph Simplification

The data-flow graph we collect is necessarily large in order to capture a complete representation of a program's behavior. Figure 1a shows a 100 instruction snapshot of the recorded data-flow from a CryptoNight mining algorithm, which is around 5% of the complete trace used in the experiment. The snapshot considers the three instructions of interest that are executed within the time frame and records data-flow between them. Although the graph is massive, we recognize repeated patterns that correspond to the iterations of the mining algorithm. In order to generate a fingerprint of a program's data-flow, we propose a graph simplification technique that exploits these repetitions to create a compact signature that captures the instruction-level behavior of a program. The key idea in our approach is to merge isomorphic substructures located at the same depth within the graph until we have a minimal representation of the data-flow. First, we formally define the repeated substructures, and then we introduce a random walk-based approximation to efficiently compute the simplification.

▶ **Definition 1** (Rooted Subgraph)**.** *Let $G = (V, E)$ be a directed acyclic graph. A subgraph $S \subseteq G$ is a* ***rooted subgraph*** *if there exists $v \in V(S)$ such that every vertex in S is reachable from v. This v is unique when G is acyclic and is called the* ***root*** *of the subgraph. S is* ***maximal*** *if it is the largest subgraph with root v.*

The isomorphic *maximal rooted subgraphs* represent repeated substructures that we want to eliminate in the simplified graphs, but isomorphic subgraphs might appear at different locations in the program that are semantically different. To preserve this distinction, we introduce the notion of *depth* which describes where a rooted subgraph S is located within the graph G and refrain from merging subgraphs located at different depths. Note that the *depth* of a rooted subgraph is an external property of S inside the graph G and is not related to its construction.

▶ **Definition 2** (Depth)**.** *The* ***depth*** *of a vertex $v \in V(G)$ is the number of edges on the longest path in G that ends in v. The depth of a rooted subgraph in G is the depth of the root vertex of the subgraph in G.*

Intuitively, the depth of a rooted subgraph contains information about the location and sequence of the corresponding instruction in the program that should be preserved in the simplified graph. Figure 3a shows many maximal isomorphic rooted subgraphs located at the same depth in the CryptoNight algorithm with the roots highlighted. These subgraphs represent the same computation carried out in different iterations of the algorithm. Finally, we iteratively merge all maximal isomorphic rooted subgraphs with distinct roots of the same depth until we reach a fixed point. Note that there is effectively no difference between merging the entire subgraph and only merging the roots since we merge until reaching a fixed point. Figure 3 shows this process on a smaller version of the CryptoNight graph. The graph shown in Figure 3a shows the center and a few branches of the large circular structure seen in the original CryptoNight graph in Figure 1a. Figure 3e is related to Figure 1e but not exactly the same due to the approximation method we introduce in the next section.

4.2.1 Approximation Through Backward Random Walks

The process of simplifying the graph requires us to search for isomorphic subgraphs in large data-flow graphs. While a naive algorithm may perform exact subgraph matching, it would be intractable because the subgraph isomorphism problem is NP-complete [22]. For reference, the graphs in our experiment have up to 1000 nodes and 2000 edges. To reduce the complexity of the simplification process, we introduce an approximate algorithm that simplifies graphs using backward random walks. Intuitively, when walking backwards randomly on a graph starting from a random vertex, the probability of a specific vertex being visited is largely dependent on the structure and size of its descendants. By computing the probability of a random backward walk visit, we get an approximate characterization of the maximal rooted subgraph of a vertex.

▶ **Definition 3** (Backward Random Walk)**.** *A* ***backward walk*** *is a sequence of vertices*

$$P = \{v_1, v_2, ..., v_k | v_i \in V(G) \text{ for } 1 \leq i \leq k\}$$

such that there exists an edge $e = v_{i+1} \rightarrow v_i$ for $1 \leq i \leq k-1$, and v_k has no incoming edge. The backward walk visits vertices in the opposite direction of the edges (i.e. $v_1, v_2, ..., v_k$).

Since the graph is acyclic, each vertex is visited at most once per backward walk. Denote $P(v)$ the probability that a vertex $v \in V(G)$ is visited in a backward random walk. The following lemma establishes a connection between the backward random walk and the maximal rooted subgraphs.

▶ **Lemma 4.** *Let G be a directed acyclic graph with no multi-edges. The probability that a vertex $v \in V(G)$ is visited in a random backward walk is*

$$P(v) = \frac{1}{|V(G)|} + \sum_{v_c \in C(v)} \frac{1}{|I(v_c)|} P(v_c)$$

where $C(v)$ denotes the set of children vertices of v in the directed graph and $|I(v_c)|$ denotes the number of incoming edges into v_c.

The intuition behind Lemma 4 is that, given that a backward walk W contains v, either: (1) v is the first vertex in the backward walk; or (2) the backward walk visits a child of v then proceeds (backward) to v itself. Therefore, the probability of visiting v can be decomposed to the probability that its children will be visited.

Proof. Consider a backward random walk W. Let E_0 denote the event that v is the first vertex in the backward walk W. Denote $v_{c_1}, v_{c_2}, ..., v_{c_M} \in C(v)$ the children vertices of v. Let E_i for $1 \leq i \leq M$ denote the event that the backward walk visits v_{c_i} and then v consecutively. Then the event that $v \in W$ is

$$E(v \in W) = E_0 \cup \bigcup_{i=1}^{M} E_i$$

In other words, v is in W if and only if W starts with v, or W visits a child of v and proceeds to v. It is clear that E_0 is mutually exclusive to every E_i where $i \neq 0$. Moreover, every E_i for $1 \leq i \leq M$ is mutually exclusive, since if two E_i and E_j are true for $i \neq j$, the graph would contain a cycle. So that

$$P(v \in W) = P(E_0) + \sum_{i=1}^{M} P(E_i) = \frac{1}{|V(G)|} + \sum_{v_c \in C(v)} \frac{1}{|I(v_c)|} P(v_c)$$ ◀

Lemma 4 implies that the probability that a vertex is visited in a random backward walk is characterized entirely by its maximal rooted graph. We state this formally next.

▶ **Theorem 5.** *Let $H_1, H_2 \subseteq G$ be maximal isomorphic rooted subgraphs such that every pair of isomorphic vertices in H_1 and H_2 contains the same number of incoming edges in G. Then the roots $v_1 \in H_1$ and $v_2 \in H_2$ have the same probability of being visited in a random backward walk.*

To prove this theorem, we need the following short lemma.

▶ **Lemma 6.** *Every path of the longest length in a maximal rooted subgraph $H \subseteq G$ contains the root vertex.*

Proof. Let $P = \{v_1, v_2, ..., v_n\}$ be an arbitrary path in H such that the root vertex v is not in P. Since v is the root, there exists a path P' from v to v_1. Since H is acyclic, P' cannot intersect P, otherwise we can form a cycle. Therefore, we can form a new path by concatenating P' and P which is longer than P and contains v, proving the lemma. ◀

Proof of Theorem 5. We proceed by induction on the length N of the longest path in H_1 and H_2.
Base: When $N = 0$, H_1 and H_2 are singleton graphs. Thus

$$P(v_1) = P(v_2) = \frac{1}{|V(G)|}$$

Induction: Since H_1 and H_2 are isomorphic, the sets $C(v_1)$ and $C(v_2)$, the children of the corresponding root vertices, are also isomorphic. Consider two isomorphic children $c_1 \in C(v_1)$ and $c_2 \in C(v_2)$. Each of these two vertices induce a maximal rooted subgraph H_1' and H_2' which are also isomorphic. Moreover, H_1' and H_2' are subgraphs of H_1 and H_2 which do not contain the roots v_1 and v_2, thus, the longest path in H_1' and H_2' is at most $N - 1$ by Lemma 6. By the induction hypothesis, $P(c_1) = P(c_2)$ for all isomorphic pair, $c_1 \in C(v_1)$ and $c_2 \in C(v_2)$. Finally, since we assume that every pair of isomorphic vertices in H_1 and H_2 contains the same number of incoming edges in G, $|I(c_1)| = |I(c_2)|$ as well for such pairs. Therefore,

$$P(v_1) = \frac{1}{|V(G)|} + \sum_{c_1 \in C(v_1)} \frac{1}{|I(c_1)|} P(c_1) = \frac{1}{|V(G)|} + \sum_{c_2 \in C(v_2)} \frac{1}{|I(c_2)|} P(c_2) = P(v_2)$$ ◀

Approximate Simplification Algorithm

Theorem 5 tells us that much of the structural information in the subgraphs is embedded in the roots in a backward random walk. It is possible that distinct non-isomorphic maximal rooted subgraphs may coincide with the same root vertex probability, or that isomorphic subgraphs may result in different root probabilities if some of the vertices have different numbers of incoming edges. We expect this to happen rarely because the regularity of this type of graphs as seen in Figure 1a implies that the structures in the graphs are not diverse and hence unlikely to collide in such a manner. It is justifiable by Theorem 5 that we can approximately merge all maximal isomorphic rooted subgraphs by combining all vertices with the same random backward walk probabilities. As it does not matter whether we merge the entire subgraph or just the root, the process is straightforward. Algorithm 1 details the overall process. Figure 1e shows the result of applying Algorithm 1 to the CryptoNight graph. More examples of simplified graphs are shown in Figure 4.

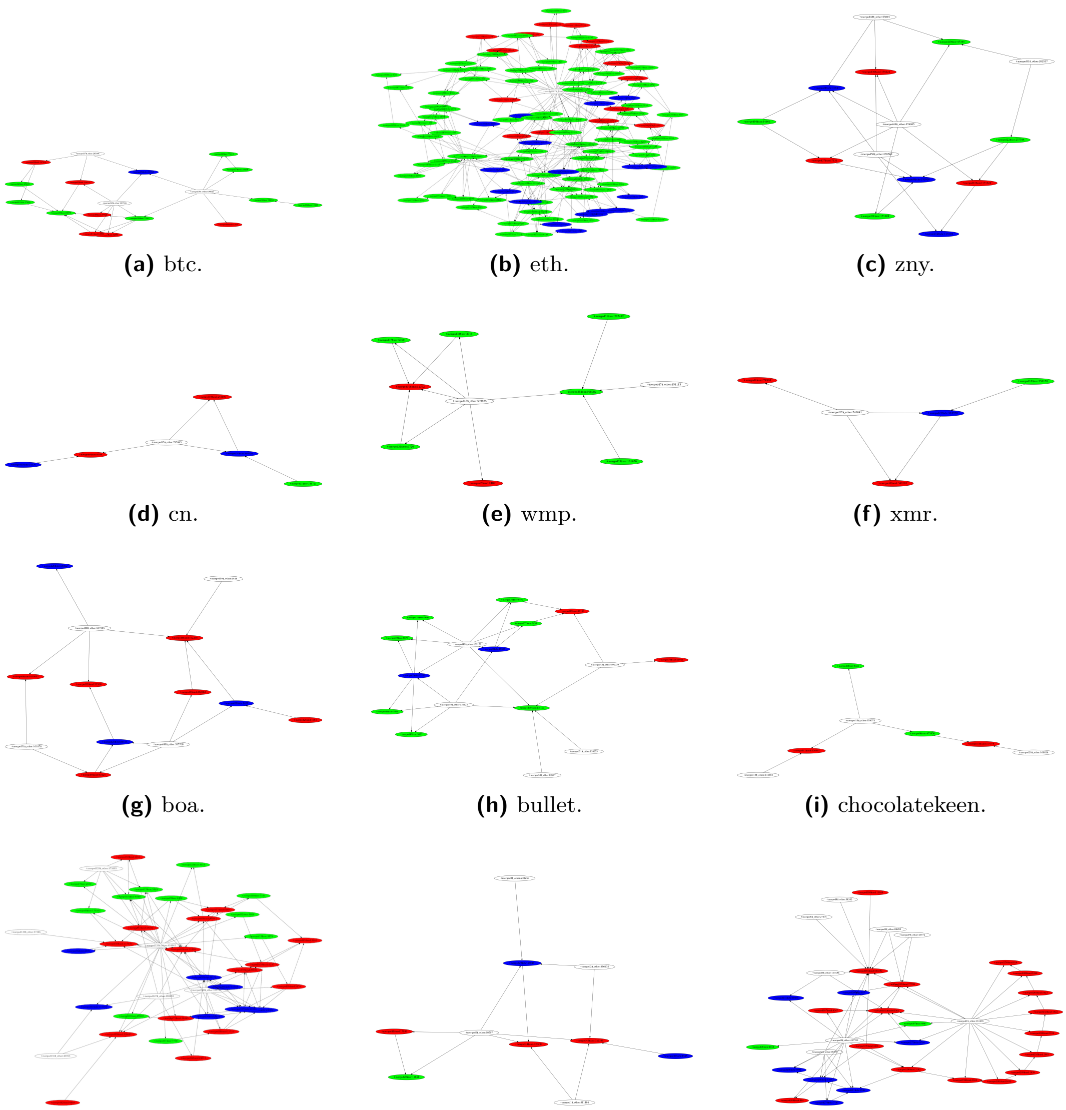

(a) btc. **(b)** eth. **(c)** zny.

(d) cn. **(e)** wmp. **(f)** xmr.

(g) boa. **(h)** bullet. **(i)** chocolatekeen.

(j) ffmpeg. **(k)** sandspiel. **(l)** sqlgui.

Figure 4 (Simplified Graphs of Miners and Non-miners) The simplified graphs of the cryptominers in (a)–(f) and 6 real-world web applications in (g)–(l). The sample details are in Table 1 and Table 2. Red, green, and blue represent `and`, `xor`, and `shr` instructions respectively. Other instructions are not traced but may appear as data origin in the graph uncolored.

Algorithm 1 Approximate Graph Simplification.

```
Input Large graph G
Output Simplified graph G
Do random backward walks to approximate the probability P(v)
for d = 0 to max depth in G do
    S ← All vertices of depth d in G
    C = {S_1, S_2, ..., S_n} ← Cluster S by P(v) using mean shift clustering
    G ← merge all vertices of the same label within the same cluster
end for
```

Quality of Approximation

Although it is difficult to give a general bound for the approximation, we can show the quality of approximation for small graphs by constructing and enumerating all approximately and exactly simplified graphs. We define approximately and exactly simplified graphs as graphs that are fixed points of the approximate and exact simplification algorithms, respectively. In other words, a simplified graph is one that cannot be simplified further by merging isomorphic subgraphs in the exact case and one that does not have vertices of the same visit probability at the same depth for the approximate case. We first construct the class of graphs G_N which contains all approximately and exactly simplified graphs of depth N as subgraphs.

▶ **Definition 7.** *Denote S_i the set of all vertices of depth $N - i$ in G_N. We construct G_N as follows. Note that G_N is a directed acyclic graph with maximum vertex depth N by the following construction.*

- *S_0 has a single vertex which contains no outgoing edges.*
- *S_i contains vertices which point to any combination of vertices with higher depth, or equivalently vertices in $\bigcup_{j=0}^{i-1} S_j$. It follows that $|S_i| = |P(\bigcup_{j=0}^{i-1} S_j)|$ where P denotes the power set. The power set $P(\bigcup_{j=0}^{i-1} S_j)$ are the sets of children of each element of S_i.*

Figure 5 shows the construction of G_3. Note that $|S_3| = 2048$ and $|S_4| = 2^{2059}$. The next theorems show that G_N contains all approximately simplified graphs and exactly simplified graphs of maximum depth N.

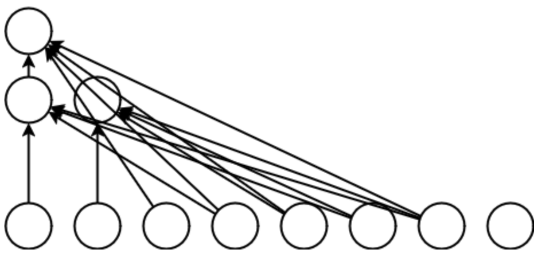

Figure 5 Visualization of G_3 in Definition 7.

▶ **Theorem 8.** *Let H be a directed acyclic (exact) simplified graph of maximum depth N. Then $H \subseteq G_N$.*

Proof. Consider a directed acyclic simplified graph H with maximum vertex depth N. Note that all vertices of depth n can only have children of depth at least $n + 1$. It follows that at depth N, every rooted subgraph is a singleton, thus there can only be one vertex of depth

N since H is simplified. Therefore S_0 has a single vertex which contains no outgoing edges, satisfying the first condition of G_N. Moreover, since every vertex can only have children of greater depth, the second condition of G_N is satisfied. Thus, $H \subseteq G_N$ ◀

▶ **Theorem 9.** *Let H be a directed acyclic approximately simplified graph of maximum depth N. Then $H \subseteq G_N$.*

Proof. The proof is mostly the same as that of Theorem 8. The only difference is that all vertices of depth N must have the same backward random walk probabilities since they have no outgoing edges, thus they must all be merged, and so $|S_0| = 1$, proving the theorem. ◀

Denote $\mathbb{H}_4$ the set of all subgraphs $H \subseteq G_4$ with $|V(H)| \leq 80$. Denote $\mathbb{A}_4$ the set of all approximately simplified graphs A with depth at most 4 and $|V(A)| \leq 80$. Denote $\mathbb{E}_4$ the set of all (exact) simplified graphs E with depth at most 4 and $|V(E)| \leq 80$. By the two theorems above, $\mathbb{A}_4 \subseteq \mathbb{H}_4$ and $\mathbb{E}_4 \subseteq \mathbb{H}_4$. Using Definition 7, we can construct the elements of $\mathbb{H}_4$. By random sampling $\mathbb{H}_4$, we can show that about 90% of all $H \in \mathbb{H}_4$ are also in $\mathbb{A}_4$. Each element of $\mathbb{H}_4$ also contains an average of 6.7 isomorphisms between maximal rooted subgraphs. These numbers are computed by inspecting a large random sample of $\mathbb{H}_4$. Intuitively, this means that, for small graphs, the approximate simplification is close to the exact simplification. Conversely, since 90% of all $H \in \mathbb{H}_4$ are in $\mathbb{A}_4$, and $\mathbb{E}_4 \subseteq \mathbb{H}_4$, it is highly likely most exact simplified graphs are fixed points for the approximate algorithm, implying that the approximate simplifying algorithm will arrive at a non-trivial solution. These bounds are relevant since almost all graphs in our experiment satisfy the condition of having depth at most 4 and at most 80 vertices.

Grouping Vertices

While the true probability of visiting a vertex in a random backward walk can be computed, we chose to give an approximation by performing the random backward walk a large number of times to tolerate noises in the graph. Since this approximation contains slight variations from the true value, we need a method to group vertices which are close in probability. Suppose that we execute the random backward walk N times, the number of times a vertex v is visited is a binomial distribution $M_v \sim B(N, P(v))$. Therefore, we can use known binomial confidence intervals to cluster the frequencies given by the random backward walk. In our implementation, we chose to use simple mean shift clustering [61] on the frequencies of the vertices to achieve a similar result.

4.3 Comparing Graph Fingerprints

Once we have generated a database of malicious graph fingerprints, we proceed to check whether a sample program contains malicious behavior. Equivalently, the sample program's fingerprint must be checked for traces of any malicious subgraphs. To achieve this, we require a subgraph similarity measure with the following characteristics:

- Able to identify shared local behavior corresponding to short sections of computation.
- Tolerates fragmentation and noise in the target super-graph which may appear naturally or due to obfuscation.
- Performs well on medium to large graphs.

In practical scenarios, there are many sources that may introduce noises to the data-flow graph. Since we capture only a brief slice of the program, two traces may capture different parts of the computation unequally. More importantly, various obfuscation techniques can

Algorithm 2 Approximate n-$\mathrm{FIS}_G(H)$.

```
Input H, G, n, k
Output approximate n-FIS_G(H)
score ← 0
for i = 1 to k do
    S ← random connected subgraph of H with n edges
    if S ⊆ G then
        score ← score + 1
    end if
end for
return score/k
```

change or remove instructions and flow control, dramatically changing certain parts of the graph. Figure 1 shows the graphs of the CryptoNight mining algorithm along with three of its obfuscated versions. Large disparities can be seen in the graphs due to insertion, deletion, and fragmentation as a result of the transformations applied to the cryptominer code. The disparities suggest that global similarity measures such as *graph edit distance* are unsuitable for comparing instruction-level data-flow graphs. The ability to tolerate noisy graphs is an important consideration in constructing a robust similarity measure.

4.3.1 Localized Fragment Similarity

A natural way to check whether a graph contains the behavior described by another graph is to look for small substructures of one graph in the other. Intuitively, we are comparing many small fragments in both graphs to search for similar segments. This idea has been employed successfully in data mining and graph databases through indexing methods based on small graph fragments [62, 71, 66]. Inspecting small fragments gives us a local view of graph similarity while being tolerant of fragmentation and noise. Moreover, searching for small subgraphs in a large graph can be done efficiently through approximations [10, 9, 8]. Based on this, we define a simple *n-fragment inclusion score* as a subgraph similarity measure.

▶ **Definition 10** (n-fragment inclusion score)**.** *The* ***n-fragment inclusion score*** *of a graph H in G, denoted n-$FIS_G(H)$, is the probability that an arbitrary connected subgraph $H' \subseteq H$ containing exactly n edges is a subgraph of G.*

Approximation

In order to avoid enumerating larger graphs and tolerate faulty results in subgraph matching, we approximate the n-FIS score by randomly testing the inclusion of a large number k of connected n-edge subgraphs. Algorithm 2 describes the approximate n-FIS score in detail. For our detection algorithm, we chose based on evaluation $n = 5$ as a compromise between locality and robustness, and $k = 500$ as a good stopping point. In order to test for subgraph inclusion, we use an open source approximate subgraph matching tool, ArcMatch [10].

Finally, we test whether a sample is malicious by computing its n-FIS score against the malicious fingerprint database. Given a fingerprint graph G of a sample, we compute the approximate n-$\mathrm{FIS}_G(H)$ for each malicious fingerprint H in the database. The existence of at least one score surpassing a threshold implies that the sample contains malicious behavior.

5 Implementation

Our implementation of PoT focuses on software running through WebAssembly. To generate data-flow graphs, we instrument programs using the open-source WebAssembly dynamic analysis tool Wasabi [43]. We use the Wasabi taint analysis framework to generate traces of data flow during execution and filter only three instructions of interest, `and`, `shr`, and `xor`.

The Wasabi analysis framework allows us to insert hooks into the programs and provide call-back functions for every executed instruction. We use these call-backs to record a trace of relevant instructions, their operands, and their results. To trace the data flow of a WebAssembly program which operates as a stack machine, we maintain a shadow stack to track the origin of each operand. Each time an instruction pushes onto the operand stack, the shadow stack stores which instruction the value originated from. Using the information tracked in the shadow stack, we are able to log the flow of data between instructions as edges between the operands and result of each instruction. A visualization of an example execution trace is shown in Figure 2. The data-flow trace is collected through the debug console as a list of data-flow edges, and the vertices in the trace are identified by the instruction that pushed the respective value onto the stack. We process this trace into the dynamic single assignment form by separating each variable into distinct generations each time it is written. Finally, we output the graph as a list of edges.

Although PoT only instruments three most relevant instructions to cryptomining, we note that the analysis and collection of data-flow traces can be extended to more instructions, which may be relevant when considering other platforms with different instruction sets.

PoT performs the following process to detect cryptomining. Given pre-processed data-flow graphs G of a sample and H of a known miner, they are simplified into fingerprint graphs G' and H' using Algorithm 1. Next, we compute 5-$\mathrm{FIS}_{G'}(H')$ using Algorithm 2 with $k = 500$ iterations. Scores are classified as malicious or benign on the basis of a static threshold. We present the reported scores and the empirical decision boundary in the evaluation section.

External Libraries

We use the Wasabi framework to instrument and perform taint analysis on Wasm binaries [43]. We use the scikit-learn library to compute the mean shift clusters in Algorithm 1. The approximate subgraph matching in Algorithm 2 uses the ArcMatch library [10].

6 Evaluation

In this section, we evaluate the following research questions.

RQ1 How effective is Algorithm 1 in simplifying large graphs?

RQ2 How effective is PoT in identifying cryptominers in the presence of obfuscation?

6.1 Experimental Setup

We ran our experiments on an 8 core AMD Ryzen 6900HX processor with 16gb memory. To evaluate our research questions, we collected a WebAssembly dataset consisting of 29 real-world web applications, 6 open-source cryptominers, and generated 39 obfuscated cryptominer samples through different obfuscations. We instrument Wasm binaries with a fork of the Wasabi framework developed by the authors of Wasm-R3 [4] at the commit version `6836ccd`.

Table 1 List of WebAssembly cryptominer samples used as evaluation targets.

Name	URL	Currency	Algorithm
btc	`https://github.com/kinshukdua/cryptominer`	Bitcoin	sha2
eth	`https://github.com/Rachel-Hu/wasm-miner`	Ethereum	ethash
zny	`https://github.com/ohac/cpuminer`	Bitzeny	yescrypt
cn	`https://github.com/andrehrferreira/cryptonight-hash`	any CryptoNight coins	CryptoNight v1
wmp	`https://github.com/notgiven688/webminerpool`	any CryptoNight coins	CryptoNight v4
xmr	`https://github.com/jtgrassie/xmr-wasm`	Monero	CryptoNight v1

Table 2 List of real-world non-miner WebAssembly web applications used in the evaluation.

Name	URL	Domain
boa	`https://boajs.dev/boa/playground`	Programming
bullet	`https://magnum.graphics/showcase/bullet`	Simulator
chocolatekeen	`https://www.jamesfmackenzie.com/chocolatekeen`	Video game
factorial	`https://www.hellorust.com/demos/factorial/index.html`	Mathematics
ffmpeg	`https://w3reality.github.io/async-thread-worker/examples/wasm-ffmpeg/index.html`	Media
figma	`https://www.figma.com`	Graphics
filament	`https://google.github.io/filament/webgl/demo_suzanne.html`	Graphics
funkykarts	`https://www.funkykarts.rocks/demo.html`	Video game
hydro	`https://cselab.github.io/aphros/wasm/hydro.html`	Simulator
imageconvolute	`https://takahirox.github.io/WebAssembly-benchmark/tests/imageConvolute.html`	Benchmark
jqkungfu	`http://jqkungfu.com`	Programming
jsc	`https://mbbill.github.io/JSC.js/demo/index.html`	Programming
mandelbrot	`http://whealy.com/Rust/mandelbrot.html`	Graphics
ogv-opus	`https://brooke.vibber.net/misc/ogv.js/demo`	Media
ogv-vp9	`https://brooke.vibber.net/misc/ogv.js/demo`	Media
onnx	`https://microsoft.github.io/onnxjs-demo/#`	ML
pacalc	`http://whealy.com/acoustics/PA_Calculator/index.html`	Mathematics
parquet	`https://google.github.io/filament/webgl/parquet.html`	Graphics
rfxgen	`https://raylibtech.itch.io/rfxgen`	Utility
rguiicons	`https://raylibtech.itch.io/rguiicons`	Utility
rguilayout	`https://raylibtech.itch.io/rguilayout`	Utility
rguistyler	`https://raylibtech.itch.io/rguistyler`	Utility
riconpacker	`https://raylibtech.itch.io/riconpacker`	Utility
rtexpacker	`https://raylibtech.itch.io/rtexpacker`	Utility
rtexviewer	`https://raylibtech.itch.io/rtexviewer`	Utility
sandspiel	`https://sandspiel.club`	Video game
sqlgui	`http://kripken.github.io/sql.js/examples/GUI`	Programming
sqlpractice	`https://www.sql-practice.com`	Programming
wasm-astar	`https://jacobdeichert.github.io/wasm-astar`	Benchmark

Cryptominers

We collected a sample of six open source `C` and `C++` miners from GitHub by searching for keywords using GitHub's search engine, e.g. "wasm", "webassembly", and "cryptominer". These searches returned 6 results after filtering out those which do not provide `C` or `C++` source code and those which do not compile. We could not use binary samples in previous works due to the lack of functional boilerplate code to execute the WebAssembly. Moreover, the obfuscators that we use in the experiment require `C` and `C++` source code for miners, which are detailed in the next section. The summary of these miners is detailed in Table 1.

Obfuscation Methods

To evaluate effectiveness against obfuscation, we found four publicly available obfuscators supporting WebAssembly which were used in previous work on WebAssembly obfuscation [11, 30]: `Tigress` [20], `emcc-obf` [30], `wasm-mutuate` [11], and `WASMixer` [12]. We found that wasm-mutate generates buggy binaries that crash at runtime due to being outdated, and many Tigress obfuscations do not work when applied alongside Wasabi instrumentation. We made the best attempt at applying the following obfuscations to as many of our sample miners as possible.

- **Tigress.** [20] (Version 4.0.10) Tigress is a source-to-source C obfuscator that has been shown to be effective in software protection [63] and evading cryptominer detection [30]. We apply the following tigress obfuscations to three of the miners which successfully ran with Tigress and Wasabi instrumentation applied.
  - **Encode Arithmetic** - Replace integer arithmetic with more complex expressions, encoded with Mixed Boolean Expressions
  - **Function Splitting and Flattening** - Splits functions into smaller fragments and removes structured control flow.
- **emcc-obf.** [30] emcc-obf is an obfuscator based on Obfuscator-LLVM [35] and the Hikari project [31]. It is implemented as middle-end passes in the LLVM toolchain. It was demonstrated to be effective in preventing reverse engineering [44] and cryptominer detection [30]. We chose the following four obfuscations which have been shown in [30] to be effective against cryptominer detection.
  - **Bogus Control flow** - Inserting spurious basic blocks and conditional jumps with opaque predicates.
  - **Control Flow Flattening** - Removes structured control flow. Similar to Tigress flattening obfuscation.
  - **Basic Block Splitting** - Splits LLVM basic blocks into multiple blocks.
  - **Substitute Instructions** - Replaces arithmetic and boolean expressions with equivalent but more complex expressions, similarly to Tigress encode arithmetic obfuscation.
- **WASMixer.** [12] WASMixer is a binary obfuscator for WebAssembly. We applied the alias disruption, control flow flattening, and memory encryption obfuscations to three of the miner samples which ran successfully with WASMixer and Wasabi instrumentation applied. The name obfuscation in WASMixer failed to run on all our samples.

Some of these obfuscation significantly changes the structure of the data-flow graph as shown in Figure 1. Therefore, it is challenging to compare the graphs, and traditional metrics such as graph edit distance are ineffective. Our results show that the *n-fragment inclusion score* is able to effectively compare these graphs.

Non-miners

To test the ability to differentiate between mining and non-mining behavior, we evaluated our method against a sample of real-world WebAssembly web applications presented by Baek et al. [4]. This data set contains a wide variety of web applications from the *Made with WebAssembly* list [67]. We exclude samples which do not run for various reasons, e.g. Wasm binaries that contain unsupported extensions for Wasabi, websites with empty graphs, runtime errors, and dead links. In total, we tested 29 real-world Wasm web applications.

To clarify the differences between our benchmarks and Wasm-R3, we included six more programs (filament, imageconvolute, ogv-opus, ogv-vp9, onnx, sqlpractice) and excluded four programs (fib, game-of-life, multiplydouble, multiplyint). Note that "pathfinding" and "guiicons" in wasm-r3 are named "wasm-astar" and "rguiicons" in our table. To account for these differences, we tested all the evaluation targets presented in the Wasm-R3 paper, including those that failed their experiments. The programs that failed their evaluation but functioned properly for our Wasabi analysis are imageconvolute, onnx, sqlpractice, and ogv (which contains ogv-opus and ogv-vp9 for audio and video decoding demos). We added "filament" to our experiments due to the lack of variety of graphics benchmarks in Wasm-R3 and the importance of graphics computations. Filament is a popular open-source graphics engine developed by Google and has over 18,000 stars on GitHub. Finally, we excluded the four programs because they produced empty data flow graphs with our Wasabi analysis, and it is difficult to ensure whether this is due to a Wasabi bug or the nature of the program itself. They would be trivially classified as non-miners regardless. We note that we used a fork of the Wasabi framework by the Wasm-R3 authors since it is already an improvement over upstream in terms of compatibility. The details of our samples are presented in Table 2. For each website, we manually instrument Wasm binaries and inject them back into the website using Google Chrome developer tools.

Baseline Comparisons

We compare our work with three state-of-the-art publications in cryptominer detection: MINOS [53], Minesweeper [42], and WASim [59]. Among recent works on cryptominer detection, these were the few with working and publicly available artifacts.

MINOS. MINOS detects cryptomining using a convolutional neural network on gray-scale image representations of WebAssembly binaries [53]. The authors of MINOS reported high detection and low false positive rates, though it has been shown that binary diversification can effectively evade MINOS [11]. We use a re-implementation of MINOS by Cabrera-Arteaga et al. [11] which has been re-trained in Cryptic Bytes [30] using a larger dataset.

Minesweeper. Minesweeper detects cryptominer binaries using a set of heuristics based on static and intrinsic features of cryptomining code [42]. The authors created a set of fingerprints for cryptographic functions by counting cryptography-related instructions and operations. WASM binaries are classified as either being a general cryptominer based on the overall instruction count, or as a CryptoNight miner based on the existence of specific cryptographic primitives, including the following cryptographic functions: Keccak (Keccak 1600-516 and Keccak-f 1600), AES, BLAKE-256, Groestl-256, and Skein-256. These cryptographic primitives are also identified by the distribution of their instruction types.

WASim. [59] WASim proposed a classification method for WebAssembly binaries using features extracted from Wasm binary files such as function sizes, export types, file attributes, and other metadata. WASim provides four different machine learning models to classify WASM binaries into 11 different categories, including cryptominers. These classifier models include neural network, support vector machine, random forest, and naive Bayes models.

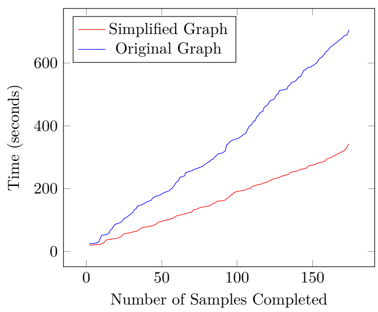

Figure 6 (Ablation Study of Analysis Time with and without Simplification) Comparison of analysis times with and without graph simplification is presented. For the original graphs, this is the time to compute Algorithm 2 (n-FIS score). For simplified graphs, the time includes both Algorithm 1 and Algorithm 2.

Table 3 A table of graph sizes for the all benchmark samples. The number of vertices and edges before and after reduction are given, as well as the percent reduction.

sample	|V|	|E|	|V'|	|E'|	-|V|%	-|E|%
btc	119	202	18	27	-84.9%	-86.6%
zny	1034	2002	14	22	-98.6%	-98.9%
cn	1326	2002	8	9	-99.4%	-99.6%
eth	1207	2002	114	276	-90.6%	-86.2%
wmp	1045	2002	11	15	-98.9%	-99.3%
xmr	1324	2002	5	5	-99.6%	-99.8%
btc-emccobf-boguscf	1037	2002	15	21	-98.6%	-99.0%
btc-emccobf-flatten	1033	2002	15	22	-98.5%	-98.9%
btc-emccobf-split	1031	2002	14	20	-98.6%	-99.0%
btc-emccobf-substitute	1065	2002	39	80	-96.3%	-96.0%
btc-tigress-encodearith	1063	2002	21	39	-98.0%	-98.1%
btc-tigress-splitflatten	1018	2002	13	18	-98.7%	-99.1%
zny-emccobf-boguscf	1111	2002	39	77	-96.5%	-96.2%
zny-emccobf-flatten	1022	2002	65	139	-93.6%	-93.1%
zny-emccobf-split	1018	2002	12	17	-98.8%	-99.2%
zny-emccobf-substitute	1067	2002	22	56	-97.9%	-97.2%
zny-tigress-encodearith	1066	2002	16	42	-98.5%	-97.9%
zny-tigress-splitflatten	1021	2002	71	153	-93.0%	-92.4%
cn-emccobf-boguscf	1336	2002	7	7	-99.5%	-99.7%
cn-emccobf-flatten	1325	2002	6	6	-99.5%	-99.7%
cn-emccobf-split	1326	2002	8	9	-99.4%	-99.6%
cn-emccobf-substitute	2191	2002	98	264	-95.5%	-86.8%
cn-tigress-encodearith	1252	2002	9	12	-99.3%	-99.4%
cn-tigress-splitflatten	1283	2002	7	10	-99.5%	-99.5%
eth-emccobf-boguscf	1212	2002	117	295	-90.3%	-85.3%
eth-emccobf-flatten	1217	2002	119	316	-90.2%	-84.2%
eth-emccobf-split	1212	2002	101	242	-91.7%	-87.9%
eth-emccobf-substitute	1505	2002	100	417	-93.4%	-79.2%
wmp-emccobf-boguscf	1049	2002	11	12	-99.0%	-99.4%
wmp-emccobf-flatten	1046	2002	11	15	-98.9%	-99.3%
wmp-emccobf-split	1039	2002	6	5	-99.4%	-99.8%
wmp-emccobf-substitute	1044	2002	12	16	-98.9%	-99.2%
xmr-emccobf-boguscf	1296	2002	16	30	-98.8%	-98.5%
xmr-emccobf-flatten	1325	2002	7	8	-99.5%	-99.6%
xmr-emccobf-split	1324	2002	5	5	-99.6%	-99.8%
xmr-emccobf-substitute	2194	2002	101	301	-95.4%	-85.0%
boa	1032	2002	13	16	-98.7%	-99.2%
bullet	179	202	16	25	-91.1%	-87.6%
chocolatekeen	104	202	7	6	-93.3%	-97.0%
factorial	1030	2002	17	27	-98.3%	-98.7%
ffmpeg	1110	1972	36	87	-96.8%	-95.6%
figma	652	1270	12	19	-98.2%	-98.5%
filament	1046	2002	9	15	-99.1%	-99.3%
funkykarts	1006	2002	7	5	-99.3%	-99.8%
hydro	1072	1878	27	63	-97.5%	-96.6%
imageconvolute	1005	2002	5	4	-99.5%	-99.8%
jqkungfu	1005	2002	5	4	-99.5%	-99.8%
jsc	1019	2002	19	29	-98.1%	-98.6%
mandelbrot	1003	2002	3	2	-99.7%	-99.9%
ogv-opus	1126	1998	21	40	-98.1%	-98.0%
ogv-vp9	1139	1888	11	16	-99.0%	-99.2%
onnx	1008	2002	3	2	-99.7%	-99.9%
pacalc	1090	2002	130	311	-88.1%	-84.5%
parquet	1046	2002	9	15	-99.1%	-99.3%
rfxgen	1032	2002	11	14	-98.9%	-99.3%
rguiicons	1057	2002	14	20	-98.7%	-99.0%
rguilayout	1041	2002	8	9	-99.2%	-99.6%
rguistyler	1041	2002	7	7	-99.3%	-99.7%
riconpacker	1030	2002	22	52	-97.9%	-97.4%
rtexpacker	1062	2002	11	16	-99.0%	-99.2%
rtexviewer	1061	2000	9	12	-99.2%	-99.4%
sandspiel	1014	2002	10	13	-99.0%	-99.4%
sqlgui	1205	1840	36	69	-97.0%	-96.2%
sqlpractice	884	1712	8	8	-99.1%	-99.5%
wasm-astar	1095	2002	34	67	-96.9%	-96.7%

Table 4 (Simplified and Unsimplified Miners Pairwise n-FIS Scores) Pairwise comparison of 5-FIS score between the miner samples with and without graph simplification. The miner in each row is checked whether it contains the miner in each column as subgraphs. Scores above 0.5 and 0.65 are highlight in light red and dark red respectively.

(a) **Simplified** Miners Pairwise n-FIS Scores

miner	btc	zny	cn	eth	wmp	xmr
btc	0.915	0.249	0.091	0.119	0.57	0.209
zny	0.121	0.929	0.163	0.057	0.275	0.207
cn	0.023	0.154	0.817	0.037	0.035	0.94
eth	0.823	0.277	0.074	0.972	0.916	0.171
wmp	0.233	0.098	0.03	0.027	0.94	0.188
xmr	0.031	0.097	0.709	0.029	0.01	1.0

(b) **Unsimplified** Miners Pairwise n-FIS Scores

miner	btc	zny	cn	eth	wmp	xmr
btc	0.851	0.236	0.151	0.221	0.484	0.184
zny	0.251	0.867	0.183	0.173	0.453	0.206
cn	0.13	0.36	0.756	0.145	0.022	0.743
eth	0.551	0.265	0.143	0.943	0.577	0.145
wmp	0.138	0.201	0.162	0.03	0.83	0.225
xmr	0.118	0.303	0.855	0.161	0.011	0.821

6.2 RQ1: The Effectiveness of Graph Simplification

To demonstrate the effectiveness of our graph simplification algorithm, Table 3 shows the reduction in the number of vertices and edges in the graphs of our benchmark samples (miners, obfuscated miners, and non-miners). Across all 65 graphs, we achieve an average of 97.3% reduction in vertex count and 96.5% reduction in edge count. The ablation study in Figure 6 shows a significant reduction in the computation time for the n-FIS score even though ArcMatch has been shown to be scalable with respect to the number of vertices and edges [10].

Table 4a and Table 4b show the n-FIS scores between each pair of cryptominers in the sample with and without graph simplification, respectively. The scores change only slightly for most entries, except for `eth`, which has a much more complex and less reducible graph than the other samples. The larger simplified graph of `eth`, which contains more than 10 times the number of edges and vertices of other samples, would make it much more prone to contain other fingerprints as a subgraph due to its size and complexity. Although the algorithm preserves structural information and connectivity, combining repeated subgraphs means that we lose most information about the frequency of the substructures, yet the scores demonstrate that this structural information is enough to differentiate between different species of miners in our sample. The detection results in Table 7 show that the complete framework of PoT achieves better accuracy and f_1 score compared to PoT without graph simplification, demonstrating that this minimal structural information is not only sufficient, but also amplifies the uniqueness of cryptominer data-flow graphs. We note that we could not complete a similar comparison as Table 4b for unsimplified non-miners because the analysis was too slow to complete without graph simplification. Despite Table 3 indicating similar numbers of vertices and edges to those of miners, we observe that the ratio of edges to vertices is significantly higher in simplified non-miners compared to simplified miners (with the exception of `eth`), suggesting higher complexity and connectivity in the non-miner graphs, which scale poorly with the ArcMatch library [10].

6.3 RQ2: The Effectiveness of PoT

To demonstrate the effectiveness of PoT and the *n-fragment inclusion score*, we test its ability to distinguish cryptomining behavior in the presence of obfuscation, as well as differentiate between miners and non-miners. Table 4a shows the n-FIS score of the miner samples against themselves. The scores reflect clear differences between the different species of miners. We observe that `cn` and `xmr` both perform the same variant of the `CryptoNight` algorithm and therefore share mutually high inclusion score. Note that the inclusion scores are not necessarily symmetric, as seen with `wmp` and `eth`. Although both algorithms use the `keccak` family of hashing algorithms as a component, they perform additional work to achieve memory-hardness [21, 73]. We hypothesize that the additional work performed by `wmp` distinct from `eth` does not include the three instrumented instructions `and`, `xor`, and `shr`, giving the impression that the work performed by `wmp` is a subset of `eth`.

The first six rows of Table 5 shows the performance of our baselines in the six miner samples. MINOS and Minesweeper are able to recognize all six samples as cryptominers, while the four models provided by WASim struggle to identify our samples.

6.3.1 Effectiveness Against Obfuscation

The first half of Table 5 shows the detection results of the six baselines in the obfuscated miner samples. Among these, Minesweeper achieved the highest sensitivity at 95.6%, followed by WASim naive Bayes, and MINOS. Although MINOS was able to detect all of our original samples as cryptominers, it struggles to identify the obfuscated samples, especially under function splitting and control flow flattening obfuscations.

The first half of Table 6 shows the n-FIS score of each obfuscated miner against the original miners. In the last column we present the PoT detection results at 0.65 score threshold for any match in the miner database. At this threshold, only 3 obfuscated samples are missed, with a sensitivity of 92.3%. The similarity trends present in Table 4a are also present in the obfuscated miner samples, with some exception. Of interest is the instruction substitution obfuscation performed by emcc-obf, which consistently raises the subgraph similarity scores for all the miner fingerprints, across all obfuscated samples. The graphs of CryptoNight with and without substitution obfuscation, shown in Figure 1b and Figure 1a respectively, suggests that the variety of substituted instructions creates a complex enough graph to contain the behavior patterns of all other miners.

6.3.2 False Positives

Finally, we evaluate the performance of the detection methods against a sample of real-world WASM web applications to test for false positives. The results for the baselines are shown in the second half of Table 5. Although WASim neural network, random forest, and support vector machine classifiers all have high specificity of 100%, 96.6%, and 89.7%, respectively, they also classify the majority of malicious samples as benign. Minesweeper on the other hand classifies almost everything as malicious, getting a 3.4% specificity.

The second half of Table 6 shows the n-FIS scores and the results for the 0.65 detection threshold for non-miners. Although we achieve a specificity of 100% at this threshold, we observe that the similarity scores are high for the `xmr` miner due to the simplicity of its data-flow graph. From this, it would be reasonable to apply different detection thresholds for different malicious fingerprint graphs based on their sizes or another simplicity metric.

Table 5 (Baseline vs. All Benchmark Samples) Baseline detection results for miners, obfuscated miners, and non-miners. 1 and 0 represent malign and benign results respectively. The columns show results for MINOS, Minesweeper, WASim neural network, WASim random forest, WASim support vector, and WASim naive bayes classifiers from left to right.

miner	obf	strat	minos	mswp	wsnn	wsrf	wssv	wsnb
zny	-	-	1	1	0	0	0	1
cn	-	-	1	1	1	1	0	0
btc	-	-	1	1	0	0	0	1
eth	-	-	1	1	0	0	0	1
wmp	-	-	1	1	0	1	0	0
xmr	-	-	1	1	1	0	0	0
btc	emccobf	boguscf	0	1	0	0	0	1
btc	emccobf	flatten	0	1	0	0	0	1
btc	emccobf	split	0	1	0	0	0	1
btc	emccobf	substitute	0	1	0	0	0	1
btc	tigress	encodearith	0	1	0	0	0	1
btc	tigress	splitflatten	1	1	0	0	0	1
zny	emccobf	boguscf	1	1	0	0	0	1
zny	emccobf	flatten	0	1	0	0	0	1
zny	emccobf	split	0	1	0	0	0	1
zny	emccobf	substitute	1	1	0	0	0	1
zny	tigress	encodearith	1	1	0	0	0	0
zny	tigress	splitflatten	0	1	0	0	0	1
cn	tigress	encodearith	1	1	0	1	0	0
cn	tigress	splitflatten	0	0	0	0	0	0
cn	emccobf	boguscf	1	1	0	1	0	0
cn	emccobf	flatten	1	0	0	1	0	0
cn	emccobf	split	1	1	1	1	0	0
cn	emccobf	substitute	0	1	1	1	0	0
eth	emccobf	boguscf	0	1	0	0	0	1
eth	emccobf	flatten	1	1	0	0	0	1
eth	emccobf	split	0	1	0	0	0	1
eth	emccobf	substitute	1	1	0	0	0	1
wmp	emccobf	boguscf	1	1	0	1	0	0
wmp	emccobf	flatten	1	1	0	1	0	1
wmp	emccobf	split	1	1	0	1	0	0
wmp	emccobf	substitute	1	1	0	1	0	1
xmr	emccobf	boguscf	1	1	0	1	0	0
xmr	emccobf	flatten	0	1	0	0	0	0
xmr	emccobf	split	1	1	1	0	0	0
xmr	emccobf	substitute	0	1	1	0	0	0
btc	wasmixer	alias	1	1	0	0	0	0
btc	wasmixer	flatten	1	1	0	0	0	1
btc	wasmixer	encrypt	1	1	0	0	0	1
eth	wasmixer	alias	1	1	0	0	0	1
eth	wasmixer	flatten	1	1	0	0	0	1
eth	wasmixer	encrypt	1	1	0	0	0	1
wmp	wasmixer	alias	1	1	0	1	0	1
wmp	wasmixer	flatten	1	1	0	1	0	1
wmp	wasmixer	encrypt	1	1	0	1	0	0
nonminer	**obf**	**strat**	**minos**	**mswp**	**wsnn**	**wsrf**	**wssv**	**wsnb**
boa	-	-	0	1	0	0	0	1
bullet	-	-	0	1	0	0	0	1
chocolatekeen	-	-	1	1	0	0	0	0
factorial	-	-	0	0	0	0	0	0
ffmpeg	-	-	0	1	0	0	0	1
figma	-	-	0	1	0	0	0	0
filament	-	-	0	1	0	0	0	1
funkykarts	-	-	0	1	0	0	0	1
hydro	-	-	0	1	0	0	0	1
imageconvolute	-	-	1	1	0	0	0	0
jqkungfu	-	-	0	1	0	0	0	0
jsc	-	-	0	1	0	0	0	1
mandelbrot	-	-	1	1	0	1	0	0
ogv-opus	-	-	0	1	0	1	0	1
ogv-vp9	-	-	0	1	0	0	0	0
onnx	-	-	0	1	1	1	0	0
pacalc	-	-	1	1	0	0	0	0
parquet	-	-	0	1	0	0	0	1
rfxgen	-	-	0	1	0	0	0	1
rguiicons	-	-	0	1	0	0	0	1
rguilayout	-	-	0	1	0	0	0	1
rguistyler	-	-	0	1	0	0	0	1
riconpacker	-	-	0	1	0	0	0	1
rtexpacker	-	-	0	1	0	0	0	1
rtexviewer	-	-	0	1	0	0	0	1
sandspiel	-	-	1	1	0	0	0	1
sqlgui	-	-	0	1	0	0	0	1
sqlpractice	-	-	0	1	0	0	0	1
wasm-astar	-	-	0	1	0	0	0	0

Table 6 (Benchmark Samples n-FIS scores) The 5-FIS scores showing the inclusion of each original miner fingerprint (columns) inside each benchmark sample (rows) is shown. The last column shows the detection result for a 0.65 5-FIS score threshold in any column. Cells above 0.5 and 0.65 scores are highlighted in light red and dark red respectively.

miner	obf	strat	btc	zny	cn	eth	wmp	xmr	≥0.65
btc	emccobf	boguscf	0.903	0.267	0.081	0.072	0.57	0.177	1
btc	emccobf	flatten	0.695	0.301	0.092	0.082	0.55	0.187	1
btc	emccobf	split	0.653	0.256	0.081	0.073	0.534	0.193	1
btc	emccobf	substitute	0.846	0.326	0.475	0.217	0.773	0.453	1
btc	tigress	encodearith	0.777	0.451	0.527	0.162	0.733	0.601	1
btc	tigress	splitflatten	0.733	0.275	0.093	0.058	0.671	0.193	1
btc	wasmixer	alias	0.665	0.265	0.081	0.061	0.531	0.205	1
btc	wasmixer	flatten	0.656	0.283	0.519	0.073	0.596	0.613	1
btc	wasmixer	encrypt	0.178	0.105	0.017	0.008	0.222	0.085	0
zny	emccobf	boguscf	0.197	0.821	0.187	0.613	0.519	0.161	1
zny	emccobf	flatten	0.224	0.783	0.211	0.619	0.499	0.154	1
zny	emccobf	split	0.145	0.821	0.157	0.069	0.545	0.064	1
zny	emccobf	substitute	0.38	0.911	0.674	0.269	0.896	0.759	1
zny	tigress	encodearith	0.38	0.307	0.511	0.059	0.804	0.598	1
zny	tigress	splitflatten	0.266	0.739	0.189	0.631	0.705	0.217	1
cn	emccobf	boguscf	0.03	0.106	0.647	0.04	0.04	0.951	1
cn	emccobf	flatten	0.031	0.092	0.748	0.044	0.024	1.0	1
cn	emccobf	split	0.038	0.151	0.836	0.039	0.029	0.945	1
cn	emccobf	substitute	0.945	0.777	0.824	0.896	0.877	0.88	1
cn	tigress	encodearith	0.029	0.197	0.792	0.063	0.087	0.735	1
cn	tigress	splitflatten	0.027	0.181	0.966	0.047	0.146	0.985	1
eth	emccobf	boguscf	0.81	0.271	0.129	0.97	0.912	0.165	1
eth	emccobf	flatten	0.801	0.358	0.057	0.967	0.886	0.099	1
eth	emccobf	split	0.801	0.339	0.068	0.967	0.909	0.181	1
eth	emccobf	substitute	0.957	0.919	0.203	0.971	0.879	0.209	1
eth	wasmixer	alias	0.832	0.334	0.073	0.966	0.891	0.153	1
eth	wasmixer	flatten	0.785	0.294	0.055	0.963	0.887	0.091	1
eth	wasmixer	encrypt	0.815	0.351	0.051	0.976	0.853	0.109	1
wmp	emccobf	boguscf	0.195	0.069	0.015	0.023	0.858	0.109	1
wmp	emccobf	flatten	0.195	0.089	0.023	0.025	0.836	0.163	1
wmp	emccobf	split	0.126	0.02	0.0	0.015	0.344	0.0	0
wmp	emccobf	substitute	0.233	0.106	0.029	0.027	0.935	0.146	1
wmp	wasmixer	alias	0.857	0.553	0.208	0.802	0.899	0.215	1
wmp	wasmixer	flatten	0.227	0.081	0.027	0.027	0.944	0.175	1
wmp	wasmixer	encrypt	0.027	0.079	0.011	0.006	0.383	0.099	0
xmr	emccobf	boguscf	0.23	0.383	0.815	0.203	0.615	0.878	1
xmr	emccobf	flatten	0.032	0.129	0.817	0.06	0.04	0.948	1
xmr	emccobf	split	0.027	0.092	0.714	0.042	0.04	1.0	1
xmr	emccobf	substitute	0.961	0.718	0.81	0.909	0.889	0.876	1
nonminer	**obf**	**strat**	**btc**	**zny**	**cn**	**eth**	**wmp**	**xmr**	**≥0.65**
boa	-	-	0.017	0.214	0.309	0.005	0.011	0.415	0
bullet	-	-	0.082	0.162	0.021	0.023	0.449	0.169	0
chocolatekeen	-	-	0.062	0.091	0.0	0.001	0.497	0.0	0
factorial	-	-	0.34	0.447	0.378	0.034	0.639	0.533	0
ffmpeg	-	-	0.366	0.558	0.382	0.069	0.573	0.569	0
figma	-	-	0.016	0.192	0.398	0.001	0.009	0.369	0
filament	-	-	0.033	0.143	0.526	0.005	0.014	0.597	0
funkykarts	-	-	0.014	0.031	0.017	0.002	0.015	0.061	0
hydro	-	-	0.138	0.377	0.373	0.033	0.412	0.539	0
imageconvolute	-	-	0.007	0.013	0.011	0.0	0.021	0.073	0
jqkungfu	-	-	0.005	0.013	0.007	0.0	0.02	0.065	0
jsc	-	-	0.058	0.244	0.239	0.006	0.347	0.291	0
mandelbrot	-	-	0.009	0.033	0.0	0.0	0.064	0.0	0
ogv-opus	-	-	0.164	0.486	0.362	0.031	0.427	0.551	0
ogv-vp9	-	-	0.1	0.37	0.494	0.018	0.119	0.602	0
onnx	-	-	0.005	0.014	0.008	0.0	0.013	0.065	0
pacalc	-	-	0.048	0.271	0.385	0.014	0.019	0.525	0
parquet	-	-	0.033	0.081	0.492	0.003	0.02	0.576	0
rfxgen	-	-	0.025	0.225	0.411	0.001	0.018	0.604	0
rguiicons	-	-	0.061	0.201	0.379	0.029	0.306	0.543	0
rguilayout	-	-	0.001	0.009	0.017	0.0	0.008	0.095	0
rguistyler	-	-	0.0	0.01	0.02	0.0	0.014	0.103	0
riconpacker	-	-	0.037	0.297	0.369	0.01	0.015	0.553	0
rtexpacker	-	-	0.059	0.113	0.019	0.004	0.473	0.093	0
rtexviewer	-	-	0.061	0.115	0.013	0.005	0.463	0.099	0
sandspiel	-	-	0.201	0.189	0.323	0.014	0.101	0.568	0
sqlgui	-	-	0.115	0.425	0.377	0.028	0.449	0.525	0
sqlpractice	-	-	0.031	0.107	0.359	0.004	0.01	0.352	0
wasm-astar	-	-	0.319	0.433	0.371	0.115	0.467	0.549	0

Table 7 Summary of performance metrics of all tested detection methods. The time column is the average time to test a sample in seconds.

Method	Accuracy	Sensitivity	Specificity	Precision	f_1-score	Time (s)
PoT	95.6%	92.3%	100.0%	100.0%	96.0%	11.9
PoT (no simplify)	89.7%	87.2%	93.1%	94.4%	90.7%	19.8
MINOS	74.3%	68.9%	82.8%	86.1%	76.5%	4.78
Minesweeper	59.5%	95.6%	3.4%	60.6%	74.1%	2.01
WASim nn	45.9%	13.3%	96.6%	85.7%	23.1%	1.24
WASim rf	55.4%	33.3%	89.7%	83.3%	47.6%	0.110
WASim svm	39.2%	0.0%	100.0%	N/A	0.0%	0.095
WASim nb	50.0%	57.8%	37.9%	59.1%	58.4%	0.099

6.3.3 Results

The summarized evaluation metrics for all the detection methods tested are shown in Table 7. PoT was able to achieve an overall accuracy of 95.6% at the 0.65 detection threshold. The best result among the baselines is MINOS with 74.3% accuracy. WASim neural network, random forest, and support vector machine classifiers skew toward labeling most samples as non-miners, while Minesweeper and WASim Bayes classifier label most samples as miners.

6.4 Discussion

The result of this evaluation shows that our graph simplification algorithm in conjunction with the n-FIS score demonstrates the ability to differentiate cryptominers from other common types of Wasm web applications based on their data-flow graphs. Moreover, we demonstrate the ability to detect cryptominers under various obfuscations, outperforming the state-of-the-art MINOS.

RQ1. In the first part of our evaluation, we showed that Algorithm 1 is able to reduce graphs of over 3000 edges and vertices to around 20 in most cases. This reduction significantly speeds up comparison operations between graphs even when employing highly scalable algorithms. Furthermore, the simplification of repetitive structural information preserves the local properties of computation and amplifies the distinction of cryptomining algorithms as evident in the results in Table 7.

RQ2. The second part of our evaluation indicates that PoT is highly effective in identifying cryptominers even in the precense of obfuscation through the use of the *n-fragment inclusion score*. Although many obfuscations are able to generate substantially different graphs, the subgraph similarity score remains high, showing that our local and fragmented view of subgraph similarity is tolerant to noise introduced by common program transformations. While the `xmr` miner exhibits high inclusion scores among benign applications, this can be attributed to the simplicity of its graph and behavior, and we recommend deploying different thresholds based on the simplicity of a fingerprint in real world scenarios.

Performance. Although performance was not the main objective of our study, Figure 6 shows that our analysis is scalable. Our current unoptimized prototype is slower than the state-of-the-art tools as shown in Table 7, but we attribute the lower runtime overheads of the other tools to the simplicity and lower accuracy of their algorithms. There are several areas in which we could reduce the analysis overhead in real-world deployment. (1) The resilience of our detection method against fragmentation allows us to collect data-flow traces at random intervals, thus instrumentation overhead could be reduced significantly. (2) We developed our prototype in Python, which could be further optimized.

Scalability and Limitations. The approximate graph simplification through backward random walks is designed to solve the scalability issue of analyzing large data-flow graphs, which we have shown to be effective on real world Wasm applications in the ablation study (Figure 6 and Table 3). Since our simplification relies on repeated structures in the graph resulting from repeated computations, programs that perform many diverse types of computation may not simplify very well, but none of our real-world benchmark programs has this issue as shown in Table 3. Another limitation of our method arises due to its similarity to traditional signature checking, namely that a database of fingerprints needs to be maintained and updated. The scalability of our detection algorithm depends on the number of unique cryptomining algorithms. Fortunately, it has been shown in literature that cryptomining scripts and algorithms are low in diversity [65, 68, 38].

Future Works. Although this study focuses on cryptojacking on the web, we hypothesize that our techniques may have wider applicability to malware detection and software classification. While we perform our experiments on the WebAssembly platform for web browsers, our theoretical framework for data-flow graph analysis uses generic data-flow properties with potential applicability to other platforms that are also susceptible to cryptojacking such as servers and data centers. Future research directions include extending our detection process to non-CPU mining and other platforms such as IoT devices and servers, especially with the emergence of server-side WebAssembly. The generality of data-flow graphs also suggests that we may be able to extend our algorithms to more general software classification tasks.

7 Conclusion

In this paper, we propose using instruction-level data-flow graphs as a valuable source of information on a program's computational behavior. We present: (1) a graph simplification algorithm to reduce the computational burden of processing large and granular data-flow graphs while preserving local substructures; and (2) a subgraph similarity measure, the *n-fragment inclusion score*, based on fragment inclusion that is robust against noise and obfuscation. Our experimental results demonstrate that the simplified graph fingerprints retain essential structural information that distinguishes proof-of-work algorithms, and the n-fragment inclusion score effectively quantifies this structural difference. The combined framework PoT achieved high accuracy against standard obfuscation, outperforming existing detection methods.

References

1 Hisham Alasmary, Aminollah Khormali, Afsah Anwar, Jeman Park, Jinchun Choi, Ahmed Abusnaina, Amro Awad, Daehun Nyang, and Aziz Mohaisen. Analyzing and detecting emerging internet of things malware: A graph-based approach. *IEEE Internet of Things Journal*, 6(5):8977–8988, 2019. doi:10.1109/JIOT.2019.2925929.

2 Blake Anderson, Daniel Quist, Joshua Neil, Curtis Storlie, and Terran Lane. Graph-based malware detection using dynamic analysis. *Journal in Computer Virology*, 7(4):247–258, 2011. doi:10.1007/s11416-011-0152-x.

3 M. Arunkumar and K. Ashokkumar. A review on cloud computing security challenges, attacks and its countermeasures. *AIP Conference Proceedings*, 3037(1):020047, April 2024. doi:10.1063/5.0196063.

4 Doehyun Baek, Jakob Getz, Yusung Sim, Daniel Lehmann, Ben L. Titzer, Sukyoung Ryu, and Michael Pradel. Wasm-r3: Record-reduce-replay for realistic and standalone webassembly benchmarks. *Proc. ACM Program. Lang.*, 8(OOPSLA2):2156–2182, 2024. doi:10.1145/3689787.

5 Ujkan Q. Bajra, Ermir Rogova, and Sefer Avdiaj. Cryptocurrency blockchain and its carbon footprint: Anticipating future challenges. *Technology in Society*, 77:102571, 2024. doi:10.1016/j.techsoc.2024.102571.

6 Shrenik Bhansali, Ahmet Aris, Abbas Acar, Harun Oz, and A. Selcuk Uluagac. A first look at code obfuscation for webassembly. In *Proceedings of the 15th ACM Conference on Security and Privacy in Wireless and Mobile Networks*, WiSec '22, pages 140–145, New York, NY, USA, 2022. Association for Computing Machinery. doi:10.1145/3507657.3528560.

7 Weikang Bian, Wei Meng, and Mingxue Zhang. Minethrottle: Defending against wasm in-browser cryptojacking. In *Proceedings of The Web Conference 2020*, pages 3112–3118, 2020. doi:10.1145/3366423.3380085.

8 Vincenzo Bonnici and Rosalba Giugno. On the variable ordering in subgraph isomorphism algorithms. *IEEE ACM Trans. Comput. Biol. Bioinform.*, 14(1):193–203, 2017. doi:10.1109/TCBB.2016.2515595.

9 Vincenzo Bonnici, Rosalba Giugno, Alfredo Pulvirenti, Dennis E. Shasha, and Alfredo Ferro. A subgraph isomorphism algorithm and its application to biochemical data. *BMC Bioinform.*, 14(S-7):S13, 2013. doi:10.1186/1471-2105-14-S7-S13.

10 Vincenzo Bonnici, Roberto Grasso, Giovanni Micale, Antonio Di Maria, Dennis Shasha, Alfredo Pulvirenti, and Rosalba Giugno. Arcmatch: high-performance subgraph matching for labeled graphs by exploiting edge domains. *Data Min. Knowl. Discov.*, 38(6):3868–3921, 2024. doi:10.1007/S10618-024-01061-8.

11 Javier Cabrera-Arteaga, Martin Monperrus, Tim Toady, and Benoit Baudry. Webassembly diversification for malware evasion. *Computers & Security*, 131:103296, 2023. doi:10.1016/j.cose.2023.103296.

12 Shangtong Cao, Ningyu He, Yao Guo, and Haoyu Wang. Wasmixer: Binary obfuscation for webassembly. In Joaquin Garcia-Alfaro, Rafał Kozik, Michał Choraś, and Sokratis Katsikas, editors, *Computer Security – ESORICS 2024*, pages 88–109, Cham, 2024. Springer Nature Switzerland. doi:10.1007/978-3-031-70896-1_5.

13 Maurantonio Caprolu, Simone Raponi, Gabriele Oligeri, and Roberto Di Pietro. Cryptomining makes noise: Detecting cryptojacking via machine learning. *Computer Communications*, 171:126–139, 2021. doi:10.1016/j.comcom.2021.02.016.

14 Domhnall Carlin, Jonah Burgess, Philip O'Kane, and Sakir Sezer. You could be mine (d): the rise of cryptojacking. *IEEE Security & Privacy*, 18(2):16–22, 2019. doi:10.1109/MSEC.2019.2920585.

15 Domhnall Carlin, Philip O'Kane, Sakir Sezer, and Jonah Burgess. Detecting cryptomining using dynamic analysis. In *2018 16th Annual Conference on Privacy, Security and Trust (PST)*, pages 1–6, 2018. doi:10.1109/PST.2018.8514167.

16 Data: The adoption rate of cryptocurrency is 43% faster than that of mobile phones and 20% faster than that of the internet. https://www.chaincatcher.com/en/article/2166659. [Accessed 10-02-2025].

17 Ramaswamy Chandramouli and Wesley Hales. A data protection approach for cloud-native applications. Technical report, National Institute of Standards and Technology, 2024.

18 Hyungmin Cho. Asic-resistance of multi-hash proof-of-work mechanisms for blockchain consensus protocols. *IEEE Access*, 6:66210–66222, 2018. doi:10.1109/ACCESS.2018.2878895.

19 CoinIMP 0Miner — coinimp.com. https://www.coinimp.com/. [Accessed 10-02-2025].

20 Christian Collberg. Home — tigress.wtf. https://tigress.wtf/index.html. [Accessed 11-02-2025].

21 Monero Community. CryptoNight - Monero Docs — docs.getmonero.org. https://docs.getmonero.org/proof-of-work/cryptonight/. [Accessed 14-02-2025].

22 Stephen A. Cook. The complexity of theorem-proving procedures. In Bruce M. Kapron, editor, *Logic, Automata, and Computational Complexity: The Works of Stephen A. Cook*, volume 43 of *ACM Books*, pages 143–152. ACM, 2023. doi:10.1145/3588287.3588297.

23 Shayan Eskandari, Andreas Leoutsarakos, Troy Mursch, and Jeremy Clark. A first look at browser-based cryptojacking. In *2018 IEEE European Symposium on Security and Privacy Workshops (EuroS&PW)*, pages 58–66. IEEE, 2018. doi:10.1109/EUROSPW.2018.00014.

24 Ryan Farell. An analysis of the cryptocurrency industry. *Wharton Research Scholars*, 130:1–23, 2015.

25 Cloud Native Computing Foundation. CNCF Annual Survey 2023 — cncf.io. https://www.cncf.io/reports/cncf-annual-survey-2023/?utm_source=the+new+stack&utm_medium=referral&utm_content=inline-mention&utm_campaign=tns+platform. [Accessed 11-02-2025].

26 Ankit Gangwal and Mauro Conti. Cryptomining cannot change its spots: Detecting covert cryptomining using magnetic side-channel. *IEEE Transactions on Information Forensics and Security*, 15:1630–1639, 2020. doi:10.1109/TIFS.2019.2945171.

27 Han Gao, Shaoyin Cheng, and Weiming Zhang. Gdroid: Android malware detection and classification with graph convolutional network. *Computers & Security*, 106:102264, 2021. doi:10.1016/j.cose.2021.102264.

28 Fábio Gomes and Miguel Correia. Cryptojacking detection with cpu usage metrics. In *2020 IEEE 19th International Symposium on Network Computing and Applications (NCA)*, pages 1–10, 2020. doi:10.1109/NCA51143.2020.9306696.

29 Andreas Haas, Andreas Rossberg, Derek L. Schuff, Ben L. Titzer, Michael Holman, Dan Gohman, Luke Wagner, Alon Zakai, and JF Bastien. Bringing the web up to speed with webassembly. *SIGPLAN Not.*, 52(6):185–200, June 2017. doi:10.1145/3140587.3062363.

30 Håkon Harnes and Donn Morrison. Cryptic bytes: Webassembly obfuscation for evading cryptojacking detection. *arXiv preprint arXiv:2403.15197*, 2024. doi:10.48550/arXiv.2403.15197.

31 GitHub - HikariObfuscator/Hikari: LLVM Obfuscator — github.com. https://github.com/HikariObfuscator/Hikari. [Accessed 12-02-2025].

32 Raymond Hill. GitHub - gorhill/uBlock: uBlock Origin - An efficient blocker for Chromium and Firefox. Fast and lean. — github.com. https://github.com/gorhill/uBlock. [Accessed 10-02-2025].

33 hoshsadiq. GitHub - hoshsadiq/adblock-nocoin-list: Block lists to prevent JavaScript miners — github.com. https://github.com/hoshsadiq/adblock-nocoin-list. [Accessed 10-02-2025].

34 Xin Hu, Tzi-cker Chiueh, and Kang G. Shin. Large-scale malware indexing using function-call graphs. In *Proceedings of the 16th ACM Conference on Computer and Communications Security*, CCS '09, pages 611–620, New York, NY, USA, 2009. Association for Computing Machinery. doi:10.1145/1653662.1653736.

35 Pascal Junod, Julien Rinaldini, Johan Wehrli, and Julie Michielin. Obfuscator-LLVM – software protection for the masses. In Brecht Wyseur, editor, *Proceedings of the IEEE/ACM 1st International Workshop on Software Protection, SPRO'15, Firenze, Italy, May 19th, 2015*, pages 3–9. IEEE, 2015. doi:10.1109/SPRO.2015.10.

36 Conor Kelton, Aruna Balasubramanian, Ramya Raghavendra, and Mudhakar Srivatsa. Browser-based deep behavioral detection of web cryptomining with coinspy. In *Workshop on measurements, attacks, and defenses for the web (MADWeb)*, pages 1–12. NDSS, 2020.

37 keraf. GitHub - keraf/NoCoin: No Coin is a tiny browser extension aiming to block coin miners such as Coinhive. — github.com. https://github.com/keraf/NoCoin. [Accessed 10-02-2025].

38 Amin Kharraz, Zane Ma, Paul Murley, Charles Lever, Joshua Mason, Andrew Miller, Nikita Borisov, Manos Antonakakis, and Michael Bailey. Outguard: Detecting in-browser covert cryptocurrency mining in the wild. In *The World Wide Web Conference*, WWW '19, pages 840–852, New York, NY, USA, 2019. Association for Computing Machinery. doi:10.1145/3308558.3313665.

39 Minseo Kim, Hyerean Jang, and Youngjoo Shin. Avengers, assemble! survey of webassembly security solutions. In *2022 IEEE 15th International Conference on Cloud Computing (CLOUD)*, pages 543–553, 2022. doi:10.1109/CLOUD55607.2022.00077.

40 Joris Kinable and Orestis Kostakis. Malware classification based on call graph clustering. *Journal in Computer Virology*, 7(4):233–245, 2011. doi:10.1007/s11416-011-0151-y.

41 Oliver Knight. 'Cryptojacking' in Financial Sector Has Risen 269Year, SonicWall Says — coindesk.com. https://www.coindesk.com/business/2022/07/26/cryptojacking-in-financial-sector-has-risen-269-this-year-sonicwall-says. [Accessed 10-02-2025].

42 Radhesh Krishnan Konoth, Emanuele Vineti, Veelasha Moonsamy, Martina Lindorfer, Christopher Kruegel, Herbert Bos, and Giovanni Vigna. Minesweeper: An in-depth look into drive-by cryptocurrency mining and its defense. In *Proceedings of the 2018 ACM SIGSAC Conference on Computer and Communications Security*, CCS '18, pages 1714–1730, New York, NY, USA, 2018. Association for Computing Machinery. doi:10.1145/3243734.3243858.

43 Daniel Lehmann and Michael Pradel. Wasabi: A framework for dynamically analyzing webassembly. In Iris Bahar, Maurice Herlihy, Emmett Witchel, and Alvin R. Lebeck, editors, *Proceedings of the Twenty-Fourth International Conference on Architectural Support for Programming Languages and Operating Systems, ASPLOS 2019, Providence, RI, USA, April 13-17, 2019*, pages 1045–1058. ACM, 2019. doi:10.1145/3297858.3304068.

44 Kyeonghwan Lim, Jaemin Jeong, Seong-je Cho, Jongmoo Choi, Minkyu Park, Sangchul Han, and Seongtae Jhang. An anti-reverse engineering technique using native code and obfuscator-llvm for android applications. In *Proceedings of the International Conference on Research in Adaptive and Convergent Systems*, RACS '17, pages 217–221, New York, NY, USA, 2017. Association for Computing Machinery. doi:10.1145/3129676.3129708.

45 Binbin Liu, Junfu Shen, Jiang Ming, Qilong Zheng, Jing Li, and Dongpeng Xu. MBA-Blast: Unveiling and simplifying mixed Boolean-Arithmetic obfuscation. In *30th USENIX Security Symposium (USENIX Security 21)*, pages 1701–1718. USENIX Association, August 2021. URL: https://www.usenix.org/conference/usenixsecurity21/presentation/liu-binbin.

46 Ganapathy Mani, Vikram Pasumarti, Bharat Bhargava, Faisal Tariq Vora, James MacDonald, Justin King, and Jason Kobes. Decrypto pro: Deep learning based cryptomining malware detection using performance counters. In *2020 IEEE International Conference on Autonomic Computing and Self-Organizing Systems (ACSOS)*, pages 109–118, 2020. doi:10.1109/ACSOS49614.2020.00032.

47 mintme. mintMe | create your own token, monetize yourself! — mintme.com. https://www.mintme.com/. [Accessed 14-02-2025].

48 The Monero Project — getmonero.org. https://www.getmonero.org/. [Accessed 14-02-2025].

49 Mozilla. Using Web Workers - Web APIs | MDN — developer.mozilla.org. https://developer.mozilla.org/en-US/docs/Web/API/Web_Workers_API/Using_web_workers. [Accessed 14-02-2025].

50 Ujan Mukhopadhyay, Anthony Skjellum, Oluwakemi Hambolu, Jon Oakley, Lu Yu, and Richard Brooks. A brief survey of cryptocurrency systems. In *2016 14th Annual Conference on Privacy, Security and Trust (PST)*, pages 745–752, 2016. doi:10.1109/PST.2016.7906988.

51 Marius Musch, Christian Wressnegger, Martin Johns, and Konrad Rieck. New kid on the web: A study on the prevalence of webassembly in the wild. In Roberto Perdisci, Clémentine Maurice, Giorgio Giacinto, and Magnus Almgren, editors, *Detection of Intrusions and Malware, and Vulnerability Assessment*, pages 23–42, Cham, 2019. Springer International Publishing. doi:10.1007/978-3-030-22038-9_2.

52 Marius Musch, Christian Wressnegger, Martin Johns, and Konrad Rieck. Thieves in the browser: Web-based cryptojacking in the wild. In *Proceedings of the 14th International Conference on Availability, Reliability and Security*, pages 1–10, 2019. doi:10.1145/3339252.3339261.

53 Faraz Naseem Naseem, Ahmet Aris, Leonardo Babun, Ege Tekiner, and A Selcuk Uluagac. Minos: A lightweight real-time cryptojacking detection system. In *NDSS*, 2021.

54 Helio N. Cunha Neto, Martin Andreoni Lopez, Natalia C. Fernandes, and Diogo M. F. Mattos. Minecap: super incremental learning for detecting and blocking cryptocurrency mining on software-defined networking. *Annals of Telecommunications*, 75(3):121–131, 2020. doi:10.1007/s12243-019-00744-4.

55 Younghee Park, Douglas Reeves, Vikram Mulukutla, and Balaji Sundaravel. Fast malware classification by automated behavioral graph matching. In *Proceedings of the Sixth Annual Workshop on Cyber Security and Information Intelligence Research*, CSIIRW '10, New York, NY, USA, 2010. Association for Computing Machinery. doi:10.1145/1852666.1852716.

56 Antonio Pastor, Alberto Mozo, Stanislav Vakaruk, Daniele Canavese, Diego R. López, Leonardo Regano, Sandra Gómez-Canaval, and Antonio Lioy. Detection of encrypted cryptomining malware connections with machine and deep learning. *IEEE Access*, 8:158036–158055, 2020. doi:10.1109/ACCESS.2020.3019658.

57 Tim Starks Rebecca Heilweil. Even the US government can fall victim to cryptojacking — fedscoop.com. https://fedscoop.com/cryptojacking-federal-government-agencies-usaid/. [Accessed 10-02-2025].

58 Juan D Parra Rodriguez and Joachim Posegga. Rapid: Resource and api-based detection against in-browser miners. In *Proceedings of the 34th Annual Computer Security Applications Conference*, pages 313–326, 2018. doi:10.1145/3274694.3274735.

59 Alan Romano and Weihang Wang. Wasim: Understanding webassembly applications through classification. In *Proceedings of the 35th IEEE/ACM International Conference on Automated Software Engineering*, pages 1321–1325, 2020. doi:10.1145/3324884.3415293.

60 Michele Russo, Nedim Šrndić, and Pavel Laskov. Detection of illicit cryptomining using network metadata. *EURASIP Journal on Information Security*, 2021(1):11, 2021. doi:10.1186/s13635-021-00126-1.

61 MeanShift — scikit-learn.org. https://scikit-learn.org/stable/modules/generated/sklearn.cluster.MeanShift.html. [Accessed 12-02-2025].

62 Haichuan Shang, Xuemin Lin, Ying Zhang, Jeffrey Xu Yu, and Wei Wang. Connected substructure similarity search. In Ahmed K. Elmagarmid and Divyakant Agrawal, editors, *Proceedings of the ACM SIGMOD International Conference on Management of Data, SIGMOD 2010, Indianapolis, Indiana, USA, June 6-10, 2010*, pages 903–914. ACM, 2010. doi:10.1145/1807167.1807264.

63 Anjali J. Suresh and Sriram Sankaran. A framework for evaluation of software obfuscation tools for embedded devices. In Lejla Batina and Gang Li, editors, *Applications and Techniques in Information Security*, pages 1–13, Singapore, 2020. Springer Singapore. doi:10.1007/978-981-33-4706-9_1.

64 Ege Tekiner, Abbas Acar, and A Selcuk Uluagac. A lightweight iot cryptojacking detection mechanism in heterogeneous smart home networks. In *NDSS*, 2022.

65 Ege Tekiner, Abbas Acar, A Selcuk Uluagac, Engin Kirda, and Ali Aydin Selcuk. In-browser cryptomining for good: An untold story. In *2021 IEEE International Conference on Decentralized Applications and Infrastructures (DAPPS)*, pages 20–29. IEEE, 2021. doi:10.1109/DAPPS52256.2021.00008.

66 Yuanyuan Tian, Richard C. McEachin, Carlos Santos, David J. States, and Jignesh M. Patel. SAGA: a subgraph matching tool for biological graphs. *Bioinform.*, 23(2):232–239, 2007. doi:10.1093/BIOINFORMATICS/BTL571.

67 Aaron Turner, James Milner, and Jonathan Beri. Made with WebAssembly — madewithwebassembly.com. https://madewithwebassembly.com/. [Accessed 12-02-2025].

68 Said Varlioglu, Bilal Gonen, Murat Ozer, and Mehmet Bastug. Is cryptojacking dead after coinhive shutdown? In *2020 3rd International Conference on Information and Computer Technologies (ICICT)*, pages 385–389, 2020. doi:10.1109/ICICT50521.2020.00068.

69 Wenhao Wang, Benjamin Ferrell, Xiaoyang Xu, Kevin W Hamlen, and Shuang Hao. Seismic: Secure in-lined script monitors for interrupting cryptojacks. In *Computer Security: 23rd European Symposium on Research in Computer Security, ESORICS 2018, Barcelona, Spain, September 3-7, 2018, Proceedings, Part II 23*, pages 122–142. Springer, 2018. doi:10.1007/978-3-319-98989-1_7.

70 WebAssembly – webassembly.org. https://webassembly.org/. [Accessed 14-02-2025].

71 David W. Williams, Jun Huan, and Wei Wang. Graph database indexing using structured graph decomposition. In Rada Chirkova, Asuman Dogac, M. Tamer Özsu, and Timos K. Sellis, editors, *Proceedings of the 23rd International Conference on Data Engineering, ICDE 2007, The Marmara Hotel, Istanbul, Turkey, April 15-20, 2007*, pages 976–985. IEEE Computer Society, 2007. doi:10.1109/ICDE.2007.368956.

72 Min-Hao Wu, Yen-Jung Lai, Yan-Ling Hwang, Ting-Cheng Chang, and Fu-Hau Hsu. Minerguard: A solution to detect browser-based cryptocurrency mining through machine learning. *Applied Sciences*, 12(19), 2022. doi:10.3390/app12199838.

73 Ethash Kernel. https://xilinx.github.io/blockchainacceleration/kernel_design.html. [Accessed 14-04-2025].

74 Fabian Yamaguchi, Nico Golde, Daniel Arp, and Konrad Rieck. Modeling and discovering vulnerabilities with code property graphs. In *2014 IEEE Symposium on Security and Privacy*, pages 590–604, 2014. doi:10.1109/SP.2014.44.